

We are IntechOpen, the world's leading publisher of Open Access books Built by scientists, for scientists

6,900

Open access books available

185,000

International authors and editors

200M

Downloads

Our authors are among the

154

Countries delivered to

TOP 1%

most cited scientists

12.2%

Contributors from top 500 universities



WEB OF SCIENCE™

Selection of our books indexed in the Book Citation Index
in Web of Science™ Core Collection (BKCI)

Interested in publishing with us?
Contact book.department@intechopen.com

Numbers displayed above are based on latest data collected.
For more information visit www.intechopen.com



Swarm Intelligence Based Controller for Electric Machines and Hybrid Electric Vehicles Applications

Omar Hegazy¹, Amr Amin², and Joeri Van Mierlo¹

¹Faculty of Engineering Sciences Department of ETEC- Vrije Universiteit Brussel,

²Power and Electrical Machines Department, Faculty of Engineering – Helwan University,

¹Belgium

²Egypt

1. Introduction

Swarm Intelligence in the form of Particle Swarm Optimization (PSO) has potential applications in electric drives. The excellent characteristics of PSO may be successfully used to optimize the performance of electric machines and electric drives in many aspects. It is estimated that, electric machines consume more than 50% of the world electric energy generated. Improving efficiency in electric drives is important, mainly, for two reasons: economic saving and reduction of environmental pollution. Induction motors have a high efficiency at rated speed and torque. However, at light loads, the iron losses increase dramatically, reducing considerably the efficiency. Swarm intelligence is used to optimize the performance of three applications; these applications are represented as follows:

- Losses Minimization of two asymmetrical windings induction motor
- Maximum efficiency and minimum operating cost of three-phase induction motor
- Optimal electric drive system for fuel cell hybrid electric vehicles.

In this chapter, a field-oriented controller that is based on Particle Swarm Optimization is presented. In this system, the speed control of two asymmetrical windings induction motor is achieved while maintaining maximum efficiency of the motor. PSO selects the optimal rotor flux level at each operating point. In addition, the electromagnetic torque is also improved while maintaining a fast dynamic response. A novel approach is used to evaluate the optimal rotor flux level by using Particle Swarm Optimization. PSO method is a member of the wide category of Swarm Intelligence methods (SI). The swarm intelligence is based on real life observations of social animals (usually insects), it is more flexibility and robust than any traditional optimization methods. PSO algorithm searches for global optimization for nonlinear problems with multi-objective. There are two speed control strategies explained in the next sections. These are field-oriented controller (FOC), and FOC based on PSO. The strategies are implemented mathematically and experimental. The simulation and experimental results have demonstrated that the FOC based on PSO method saves more energy than the conventional FOC method.

In this chapter, another application of PSO for losses and operating cost minimization control is presented for the induction motor drives. Two strategies for induction motor speed control are proposed. These strategies are maximum efficiency strategy (MES), based PSO, and minimum operating cost Strategy. The proposed technique is based on the principle that the flux level in a machine can be adjusted to give the minimum amount of losses and minimum operating cost for a given value of speed and load torque.

In the demonstrated systems, the powertrain components sizing and the power control strategy are the only adjustable parameters to achieve optimal power sharing between sources and optimal design with minimum cost, minimum fuel consumption, and maximum efficiency for Electric Vehicles (EVs) and Hybrid Electric Vehicles (HEVs). Their selection greatly influences the performance of the drive system in Hybrid Electric Vehicles applications. In this section, the design and power management control are investigated and optimized by using Particle Swarm Optimization.

2. Losses minimization of two asymmetrical windings induction motor

In this section, a field orientation based on Particle Swarm Optimization (PSO) is applied to control the speed of two-asymmetrical windings induction motor. The maximum efficiency of the motor is obtained by the evaluation of optimal rotor flux at each operating point. In addition, the electro-magnetic torque is also improved while maintaining a fast dynamic response. In this section, a novel approach is used to evaluate the optimal rotor flux level. This approach is based on Particle Swarm Optimization (PSO). This section presents two speed control strategies. These are field-oriented controller (FOC) and FOC based on PSO. The strategies are implemented mathematically and experimental. The simulation and experimental results have demonstrated that the FOC based on PSO method saves more energy than the conventional FOC method [Hegazy, 2006; Amin et al., 2007; Amin et al., 2009]. The two asymmetrical windings induction motor is treated as a two-phase induction motor (TPIM). It is used in many low power applications, where three-phase supply is not readily available. This type of motor runs at an efficiency range of 50% to 65% at rated operating conditions.

The conventional field-oriented controller normally operates at rated flux at any values with its torque range. When the load is reduced considerably, the core losses become so high causing poor efficiency. If significant energy savings are required, it is necessary to optimize the efficiency of the motor. The optimum efficiency is obtained by the evaluation of the optimal rotor flux level. This flux level is varied according to the torque and the speed of the operating point.

PSO is applied to evaluate the optimal flux. It has the straightforward goal of minimizing the total losses for a given load and speed. It is shown that the efficiency is reasonably close to optimal.

2.1 Mathematical model of the motor

The d-q model of an unsymmetrical windings induction motor in a stationary reference frame can be used for a dynamic analysis. This model can take in account the core losses. The d-q model as applied to TPIM is described in [Hegazy, 2006; Amin et al., 2009]. The equivalent circuit is shown in Fig. 1.

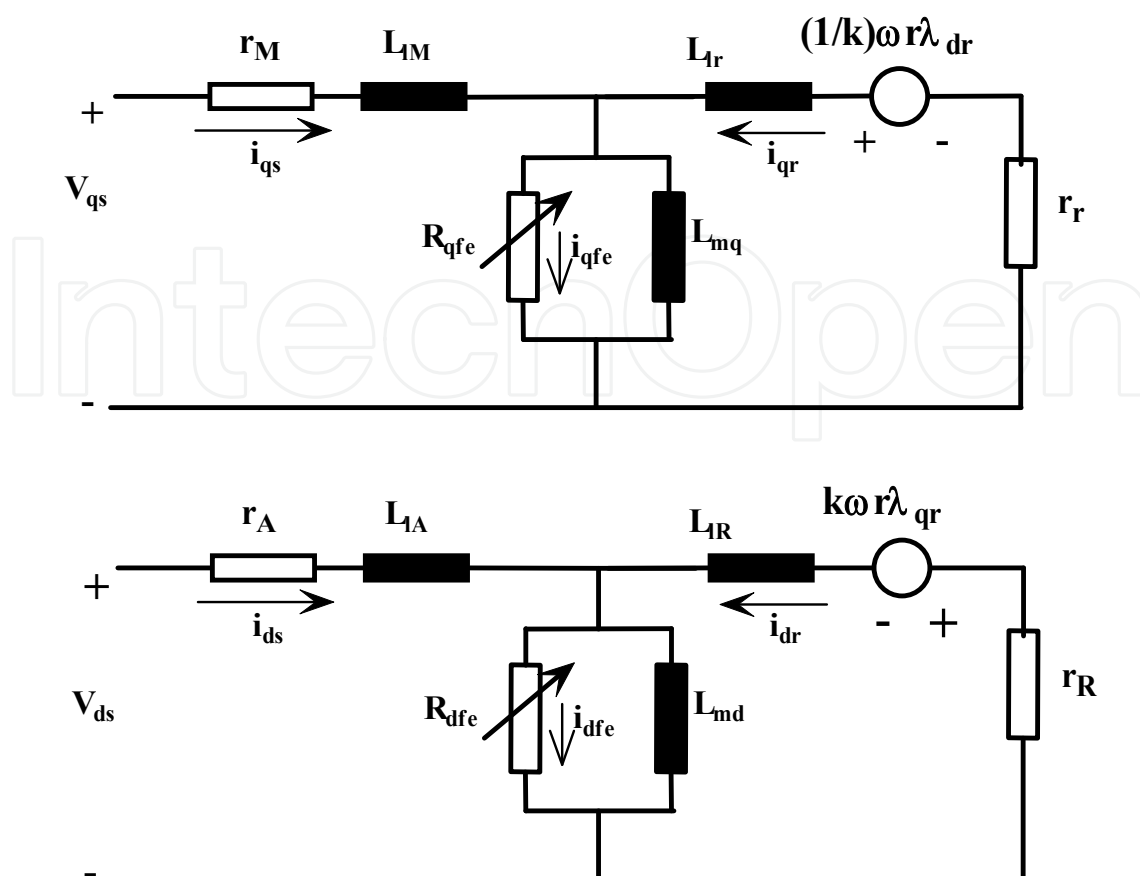


Fig. 1. The d-q axes two-phase induction motor Equivalent circuit with iron losses.

The machine model may be expressed by the following voltage and flux equations:

Voltage Equations (1):

$$v_{qs} = r_m i_{qs} + p\lambda_{qs} \quad (1)$$

$$v_{ds} = r_a i_{ds} + p\lambda_{ds} \quad (2)$$

$$0 = r_r i_{qr} - (1/k) * \omega_r \lambda_{dr} + p\lambda_{qr} \quad (3)$$

$$0 = r_R i_{ds} + k * \omega_r \lambda_{qr} + p\lambda_{dr} \quad (4)$$

$$0 = -i_{qfe} R_{qfe} + L_{mq} (p i_{qs} + p i_{qr} - p i_{qfe}) \quad (5)$$

$$0 = -i_{dfe} R_{dfe} + L_{md} (p i_{ds} + p i_{dr} - p i_{dfe}) \quad (6)$$

Flux Equations:

$$\lambda_{qs} = L_{lm} i_{qs} + L_{mq} (i_{qs} + i_{qr} - i_{qfe}) \quad (7)$$

$$\lambda_{ds} = L_{la} i_{ds} + L_{md} (i_{ds} + i_{dr} - i_{dfe}) \quad (8)$$

$$\lambda_{qr} = L_{lr} i_{qr} + L_{mq} (i_{qs} + i_{qr} - i_{qfe}) \quad (9)$$

$$\lambda_{dr} = L_{lr} i_{dr} + L_{md} (i_{ds} + i_{dr} - i_{dfe}) \quad (10)$$

Electrical torque equation is expressed as:

$$T_e = \frac{P}{2} (k L_{mq} i_{dr} (i_{qs} + i_{qr} - i_{qfe}) - \frac{1}{k} L_{md} i_{qr} (i_{ds} + i_{dr} - i_{dfe})) \quad (11)$$

$$T_e - T_l = j_m p \omega_r + B_m \omega_r \quad (12)$$

2.2 Field-Oriented Controller [FOC]

The stator windings of the motor are unbalanced. The machine parameters differ from the d axis to the q axis. The waveform of the electromagnetic torque demonstrates the unbalance of the system. The torque in equation (11) contains an AC term; it can be observed that two values are presented for the referred magnetizing inductance. It is possible to eliminate the AC term of electro-magnetic torque by an appropriate control of the stator currents. However, these relations are valid only in linear conditions. Furthermore, the model is implemented using a non-referred equivalent circuit, which presumes some complicated measurement of the magnetizing mutual inductance of the stator and the rotor circuits.

The indirect field-oriented control scheme is the most popular scheme for field-oriented controllers. It provides decoupling between the torque and the flux currents. The electric torque must be a function of the stator currents and rotor flux in synchronous reference frame [Popescu & Navrapescu, 2000]. Assuming that the stator currents can be imposed as:

$$i_{ds}^s = i_{ds1}^s \quad (13)$$

$$i_{qs}^s = k i_{qs1}^s \quad (14)$$

Where: $k = M_{srd} / M_{srq}$

$$T_e = \frac{P}{2L_r} [M_{sqr} i_{qs}^s \lambda_{dr}^s - M_{sdr} i_{ds}^s \lambda_{qr}^s] \quad (15)$$

By substituting the variables i_{ds}^s and i_{qs}^s by auxiliary variables i_{ds1}^s and i_{qs1}^s into (15) the torque can be expressed by

$$T_e = \frac{P M_{sdr}}{2L_r} [i_{qs1}^s \lambda_{dr}^s - i_{ds1}^s \lambda_{qr}^s] \quad (16)$$

In synchronous reference frame, the electromagnetic torque is expressed as:

$$T_e = \frac{P M_{sdr}}{2L_r} [i_{qs1}^e \lambda_{dr}^e - i_{ds1}^e \lambda_{qr}^e] \quad (17)$$

$$T_e = \frac{P M_{sdr}}{2L_r} [i_{qs1}^e \lambda_r^e] \quad (18)$$

$$i_{ds1}^e = \frac{\lambda_r^e}{M_{sdr}} \quad (19)$$

$$\omega_e - \omega_r = \frac{M_{sdr}}{\tau_r * \lambda_r^e} i_{qs1}^e \quad (20)$$

2.3 Synchronous reference frame for losses model

It is very complex to find the losses expression for the two asymmetrical windings induction motor with losses model. In this section, a simplified induction motor model with iron losses will be developed. For this purpose, it is necessary to transform all machine variables to the synchronous reference frame. The voltage equations are written in expanded form as follows [Hegazy, 2006; Amin et al., 2006; Amin et al., 2009]:

$$v_{qs}^e = r_m i_{qs}^e + L_{lm} \frac{di_{qs}^e}{dt} + L_{mq} \frac{di_{qm}^e}{dt} + \omega_e (L_{la} i_{ds}^e + L_{md} i_{dm}^e) \quad (21)$$

$$v_{ds}^e = r_a i_{ds}^e + L_{la} \frac{di_{ds}^e}{dt} + L_{md} \frac{di_{dm}^e}{dt} - \omega_e (L_{lm} i_{qs}^e + L_{mq} i_{qm}^e) \quad (22)$$

$$0 = r_r i_{qr}^e + L_{lr} \frac{di_{qr}^e}{dt} + L_{mq} \frac{di_{qm}^e}{dt} + \frac{\omega_{sl}}{k} (L_{lr} i_{dr}^e + L_{md} i_{dm}^e) \quad (23)$$

$$0 = r_R i_{dr}^e + L_{lR} \frac{di_{dr}^e}{dt} + L_{md} \frac{di_{dm}^e}{dt} - k * \omega_{sl} (L_{lr} i_{qr}^e + L_{mq} i_{qm}^e) \quad (24)$$

$$i_{qs}^e + i_{qr}^e = i_{qfe}^e + i_{qm}^e \quad (25)$$

$$i_{ds}^e + i_{dr}^e = i_{dfe}^e + i_{dm}^e \quad (26)$$

$$v_{dm}^e = -\frac{\omega_e L_{lr} L_{mq}}{L_r} i_{qs}^e \quad (27)$$

$$v_{qm}^e = \omega_e L_{mfs} i_{ds}^e \quad (28)$$

Where:

$$i_{dfe}^e = \frac{v_{qm}^e}{R_{qfe}}; i_{dfe}^e = \frac{v_{dm}^e}{R_{dfe}}$$

The losses in the motor are mainly:

- a. Stator copper losses,
- b. Rotor copper losses,
- c. Core losses, and

d. Friction losses

The total electrical losses can be expressed as follows

$$P_{\text{losses}} = P_{\text{cu1}} + P_{\text{cu2}} + P_{\text{core}} \quad (29)$$

Where:

P_{cu1} : Stator copper losses

P_{cu2} : Rotor copper losses

P_{core} : Core losses

The stator copper losses of the two asymmetrical windings induction motor are caused by electric currents flowing through the stator windings. The core losses of the motor are produced from the hysteresis and eddy currents in the stator. The total electrical losses of motor can be rewritten as:

$$P_{\text{losses}} = r_m i_{qs}^2 + r_a i_{ds}^2 + r_r i_{qr}^2 + r_R i_{dr}^2 + \frac{v_{qm}^2}{R_{qfe}} + \frac{v_{dm}^2}{R_{dfe}} \quad (30)$$

The total electrical losses are obtained as follows:

$$P_{\text{losses}} = \left[r_m + \frac{r_r L_{mq}^2}{L_r^2} + \frac{\omega_e^2 L_{lr}^2 L_{mq}^2}{L_r^2 R_{dfe}} \right] \left(\frac{T_e^2 L_r^2}{P^2 \left(\frac{L_{mds}}{K} \right)^2 \lambda_r^2} \right) + \left(r_a + \frac{\omega_e^2 L_{mds}^2}{R_{qfe}} \right) \frac{\lambda_r^2}{L_{mds}^2} \quad (31)$$

$$\omega_{sl} = \frac{2T_e * r_r}{P * \lambda_r^2} \quad (32)$$

Where:

$\omega_e = \omega_r + \omega_{sl}$, and ω_{sl} is the slip speed (rad/sec).

Equation (31) is the electrical losses formula, which depends on rotor flux (λ_r) according to operating point (speed and load torque). The total losses of the motor (TP_{losses}) are given as follows:

$$TP_{\text{losses}} = P_{\text{losses}} + P_{\text{Fric}} = P_{\text{in}} - P_{\text{out}} \quad (33)$$

$$\text{Efficiency } (\eta) = \frac{P_{\text{out}}}{P_{\text{out}} + TP_{\text{losses}}} \quad (34)$$

Where:

Friction power losses = $F * \omega_r^2$, and

Output power (P_{out}) = $T_L * \omega_r$.

2.4 Losses minimization control scheme

The equation (33) is the cost function, the total losses, which depends on rotor flux (λ_r) according to the operating point. Figure 2 presents the distribution of losses in motor and its variation with the flux. As the flux reduces from the rated value, the core losses decrease,

but the motor copper losses increase. However, the total losses decrease to a minimum value and then increase again. It is desirable to set the rotor flux at the optimal value, so that the efficiency is optimum [Hegazy, 2006; Amin et al., 2006; Amin et al., 2009].

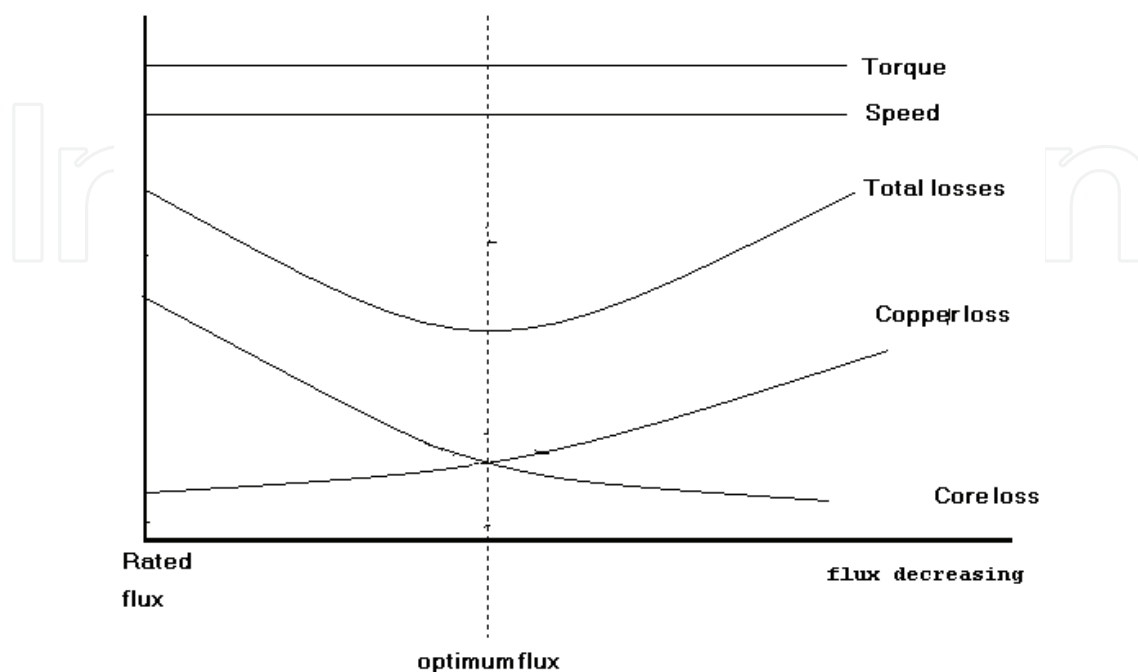


Fig. 2. Losses variation of the motor with varying flux

PSO is applied to evaluate the optimal flux that minimizes the motor losses. The problem can be formulated as follows:

$$\text{minimize } TP_{\text{losses}} = \Gamma(\lambda_r, T_L, \omega_r) \tag{35}$$

2.4.1 Particle Swarm Optimization (PSO)

Particle swarm optimization (PSO) was originally designed and introduced by Eberhart and Kennedy [Eberhart, Kennedy, 1995; Eberhart, Kennedy, 2001]. Particle Swarm Optimization (PSO) is an evolutionary computation technique (a search method based on a nature system). It can be used to solve a wide range of optimization problems. Most of the problems that can be solved using Genetic Algorithms (GA) could be solved by PSO. For example, neural network training and nonlinear optimization problems with continuous variables can be easily achieved by PSO [Eberhart, Kennedy, 2001]. It can be easily expanded to treat problems with discrete variables.

The system initially has a population of random solutions. Each potential solution, called a particle. Each particle is given a random velocity and is flown through the problem space. The particles have memory and each particle keeps track of its previous best position (call the pbest) and with its corresponding fitness. There exit a number of pbest for the respective particles in the swarm and the particle with greatest fitness is called the global best (gbest) of the swarm. PSO can be represented by the concept of velocity and position. The Velocity of each agent can be modified by the following equations: (36 & 38):

$$v^{k+1} = w v_i^k + c_1 r_1 * (pbest - s_i^k) + c_2 r_2 * (gbest - s_i^k) \tag{36}$$

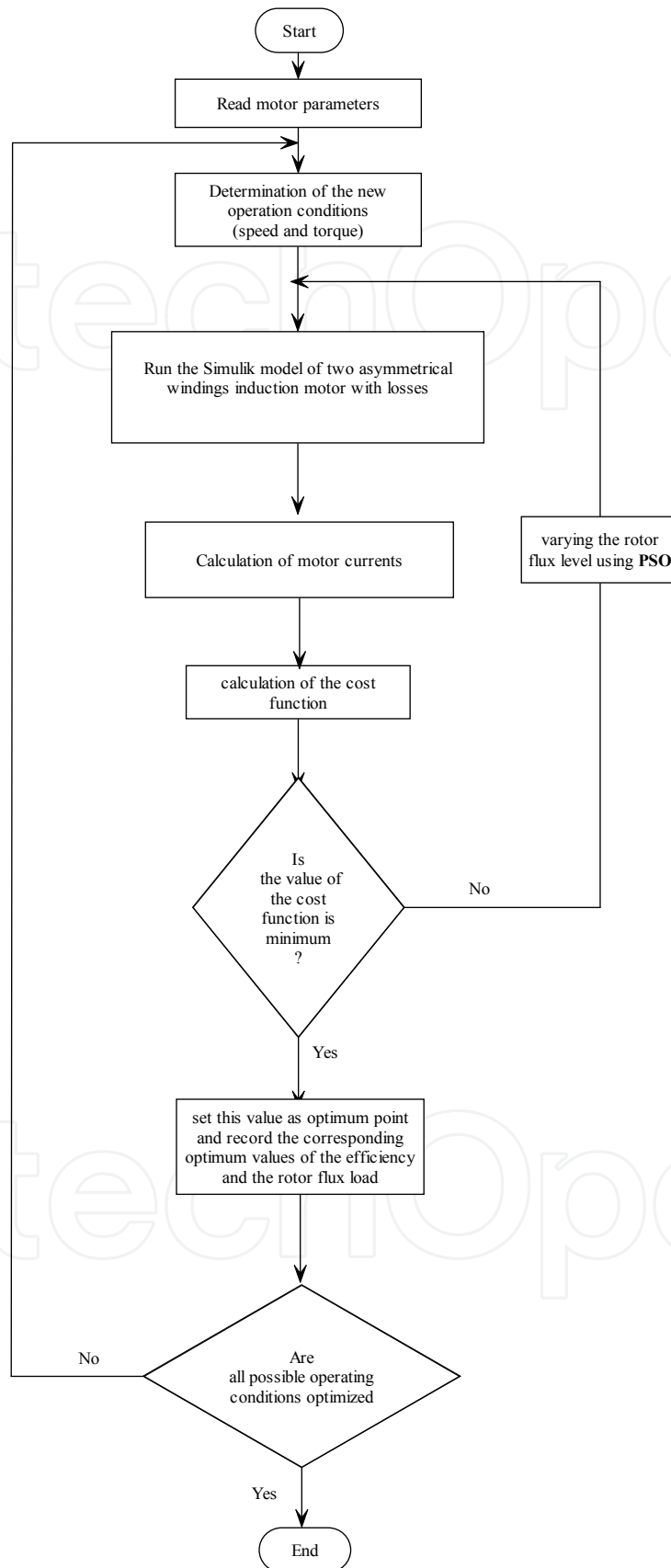


Fig. 3. The flowchart of the execution of the PSO [Hegazy, 2006]

$$\omega = \omega_{\max} - \frac{\omega_{\max} - \omega_{\min}}{\text{iter}_{\max}} * \text{iter} \quad (37)$$

Using the above equations, a certain velocity can be calculated that gradually gets close to (pbest) and (gbest). The current position (searching point in the solution space) can be modified by the following equation:

$$S_i^{k+1} = S_i^k + v_i^{k+1} \quad (38)$$

Where:

- v^k : Current velocity of agent i at iteration.
- v_i^{k+1} : Modified velocity of agent i
- r_1, r_2 : random number distributed $[0,1]$,
- S_i^k : current position of agent i ,
- ω : weight function for velocity of agent i ,
- c_1, c_2 : positive constants; $[c_1 + c_2 < 4]$.
- ω_{\max} : Initial weight,
- ω_{\min} : Final weight,
- iter_{\max} : Maximum iteration number,
- iter : Current iteration number.

- In (35), the losses formula is the cost function of the PSO. The particle swarm optimization (PSO) technique is used for minimizing this cost function.
- The PSO is applied to evaluate the optimal rotor flux that minimizes the motor losses at any operating point. Figure 3 presents the flowchart of the execution of PSO, which evaluates the optimal flux by using MATLAB /SIMULINK.

The optimal flux is the input of the indirect rotor flux oriented controller. The indirect field-oriented controller generates the required two reference currents to drive the motor corresponding to the optimal flux. These currents are fed to the hysteresis current controller of the two-level inverter. The switching pattern is generated according to the difference between the reference current and the load current through the hysteresis band. Figure 4 shows a whole control diagram of the proposed losses-minimization control system.

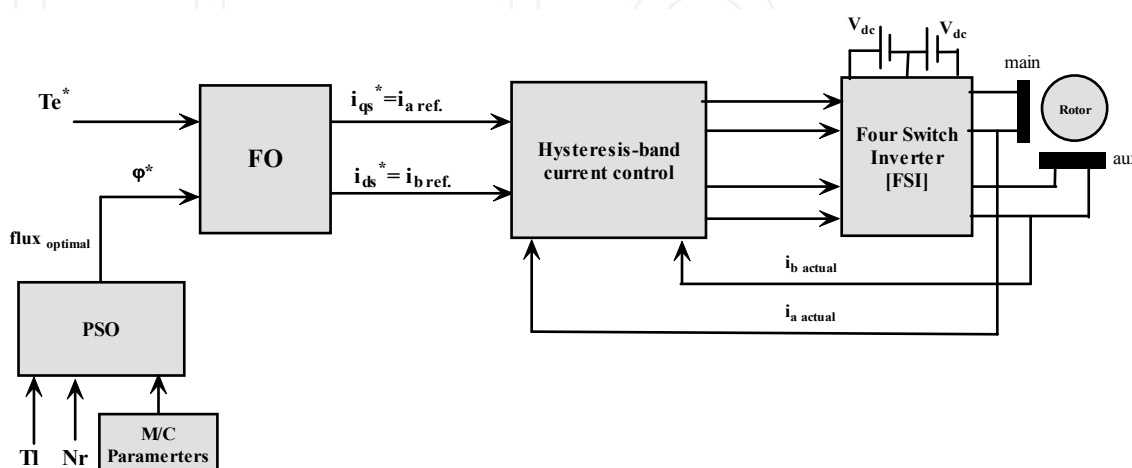


Fig. 4. The proposed losses minimization control system.

2.5 Simulation results

In this section, the proposed application is implemented numerically using MATLAB-SIMULINK to validate the performance of the proposed control strategy. The motor used in this study has the following parameters, which were measured by using experimental tests. Table 1 shows motor parameters. The used parameters of the PSO are shown in Table 2.

Rated power	750 w
V	220 v
F	50 Hz
r_M	4.6 Ω
r_A	10.6 Ω
X_{Lm}	4.31 Ω
X_{La}	7.1472 Ω
rr	3.455 Ω
X_{Lr}	4.284 Ω
X_{mq}	89.65 Ω
X_{md}	169.43 Ω
R_{qfe}	1050 Ω
R_{dfe}	1450 Ω
J	0.005776 kg.m ²
B	0.00328N.m.sec/r
Pole pair	2

Table 1. Motor Parameters

The optimal rotor flux provides the maximum efficiency at any operating point. There are six-cases of the motor operation are studied by using FOC based on PSO. PSO will evaluate the optimal rotor flux level. This flux is fed to the FOC module. Figure 5 shows the performance of the motor at case (1) ($T_L=0.25$ PU, $N_r=0.5 N_{rated}$), when PSO is applied side-by-side FOC as shown in Fig.4.

Population size	10
Max. iter	50
c1	0.5
c2	0.5
Max. weight	1.4
Min. weight	0.1
r1	[0,1]
r2	[0,1]
Lower Bound	0.2
Upper Bound	2

Table 2. PSO Algorithm parameter

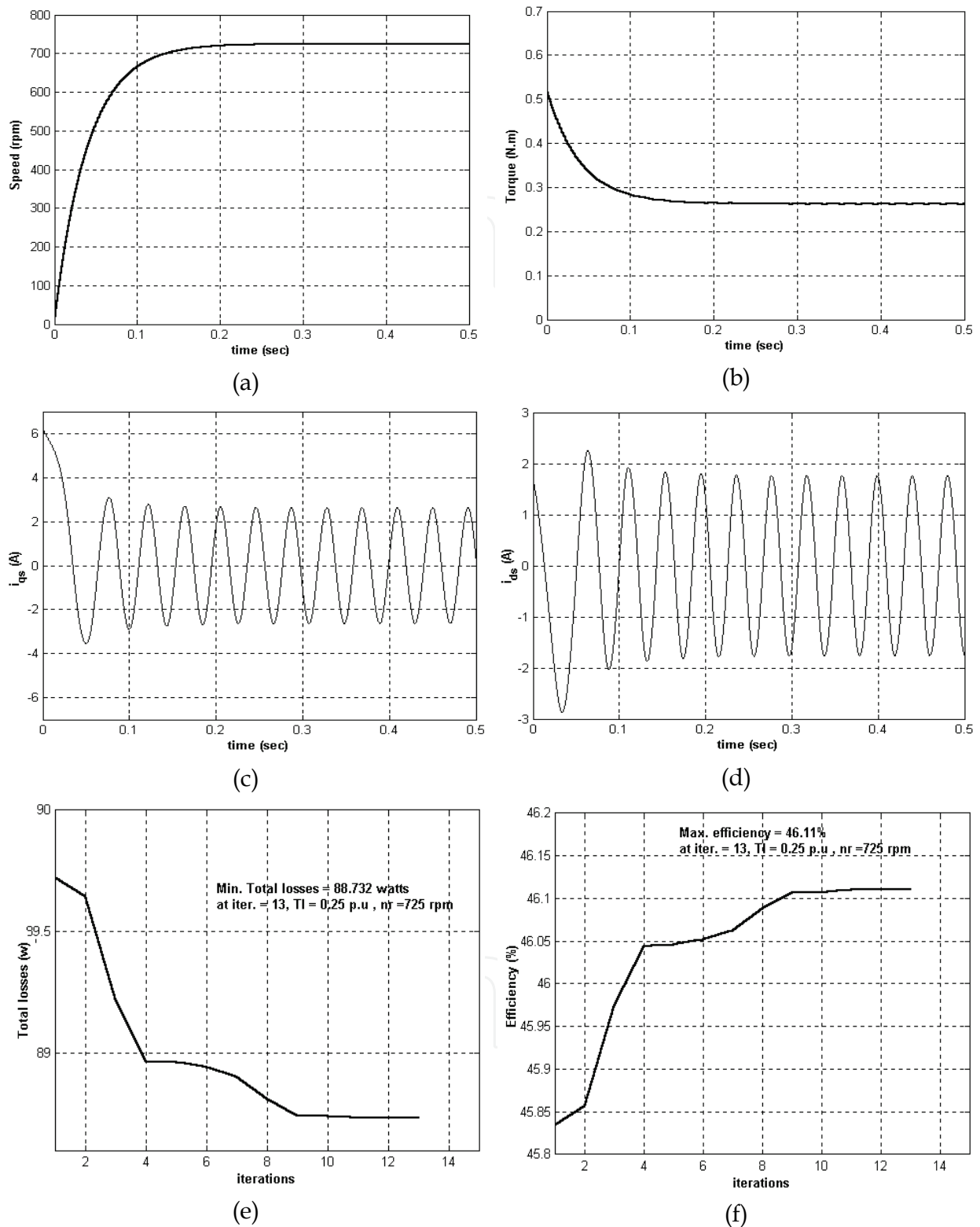


Fig. 5. Simulation results of the motor at case (1).Speed-time curve, (b) Torque-time curve, (c) The stator current in q-axis, (d) The stator current in d-axis, (e) Total Losses against iterations, (f) Efficiency against iterations

Figure 6 illustrates the comparison between FOC and FOC based PSO control methods at different operating points. Figure 7 presents the optimal flux, which is obtained by applying PSO. Table 3 presents the summary of the results of FOC and FOC based PSO methods.

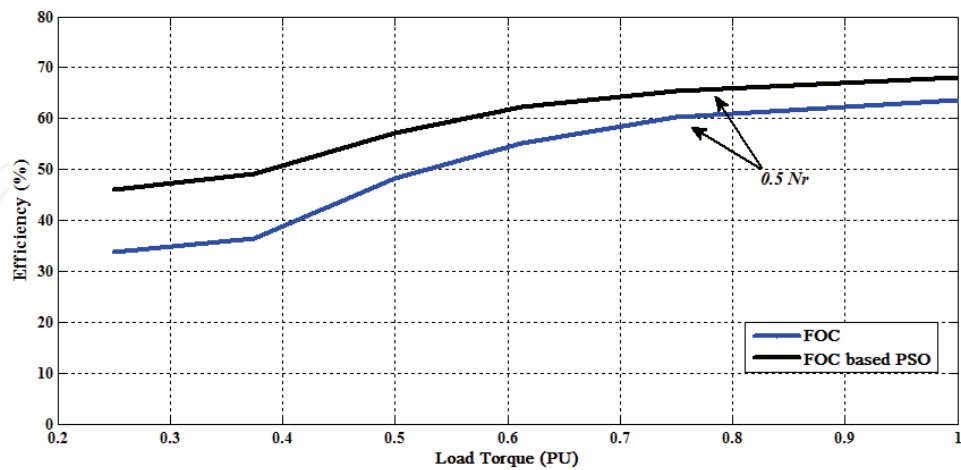


Fig. 6. the comparison between FOC and FOC based PSO

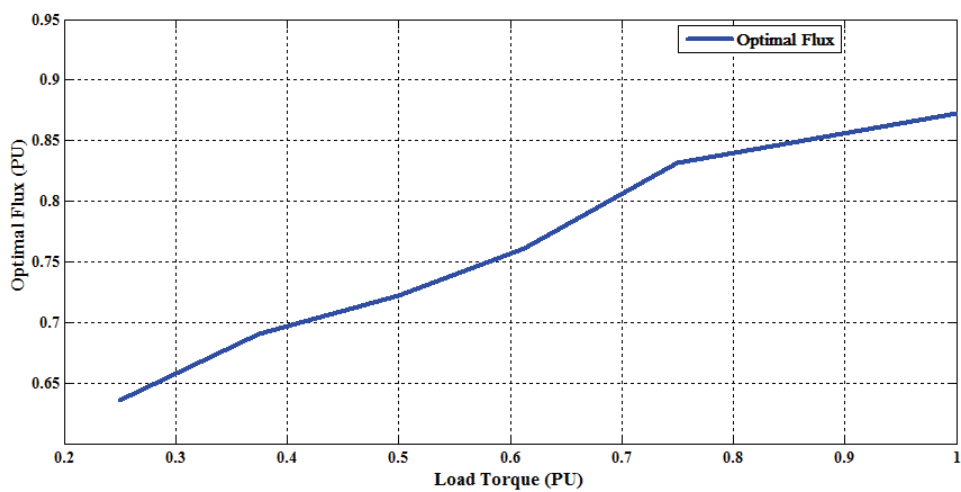


Fig. 7. The optimal flux at different load torque

Cases	T_L (PU)	N_r (rpm)	FOC		FOC based PSO		Improvement (%)
			λ (PU)	η (%)	$\lambda_{Optimal}$ (PU)	η (%)	
(1)	0.25	$0.5 N_{rated}$	1	33.85	0.636	46.11	36.22
(2)	0.375	$0.5 N_{rated}$	1	36.51	0.6906	49.15	34.62
(3)	0.5	$0.5 N_{rated}$	1	48.21	0.722	57.11	18.46
(4)	0.6125	$0.5 N_{rated}$	1	55.15	0.761	62.34	13.04
(5)	0.75	$0.5 N_{rated}$	1	60.175	0.8312	65.31	8.53
(6)	1	$0.5 N_{rated}$	1	63.54	0.8722	68.15	7.26

Table 3. Summary of the results of the two controllers

In practical system, the flux level based on PSO at different operating points (torque and speed) is calculated and stored in a look up table (LUT). The use of look up table will enable the system to work in real time without any delay that might be needed to calculate the optimal point. The proposed controller would receive the operating point (torque and speed) and get the optimum flux (λ_{optimal}) from the look up table. It will generate the required reference current. It is noticed that, the efficiency with the FOC based on PSO method is higher than the efficiency with the FOC method only.

2.6 Experimental results

To verify the validity of the proposed control scheme, a laboratory prototype is built and tested [Hegazy, 2006; Amin et al., 2006; Amin et al., 2009]. The basic elements of the proposed experimental scheme are shown in Fig. 8 and Fig. 9. The experimental results of the motor are achieved by coupling the motor to an eddy current dynamometer. The experimental results are achieved using two control methods:

- Field-Oriented Control [FOC], and
- Field-Oriented Control [FOC] based on PSO.

The reference and the actual motor currents are fed to the hysteresis current controller. The switching pattern of the two-level four-switch inverter [FSI] is generated according to the difference between the reference currents and the load currents. Figure 10 shows the experimental results of the motor with FOC at case (1), where the motor is loaded by $T_L = 0.25$ PU. Figure 11 shows the experimental result of the motor with FOC based on PSO at case (1). The cases are summarized in Table 4.

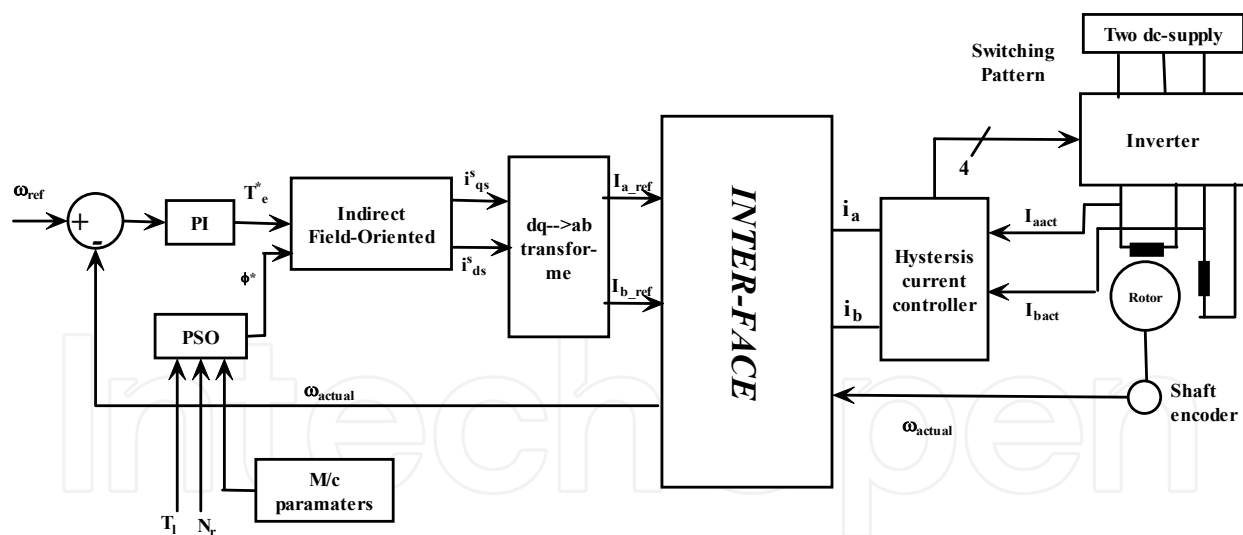


Fig. 8. Block diagram of the proposed experimental scheme [Hegazy, 2006; Amin et al., 2009]

Cases	FOC			FOC with PSO			Improvement (%)
	λ (PU)	Power Input (W)	η (%)	λ (PU)	Power Input (W)	η (%)	
(1)	1	235	32.3	0.636	169	44.92	39.07
(2)	1	323	35.2	0.690	243	47.06	33.69

Table 4. The summary of the two-cases

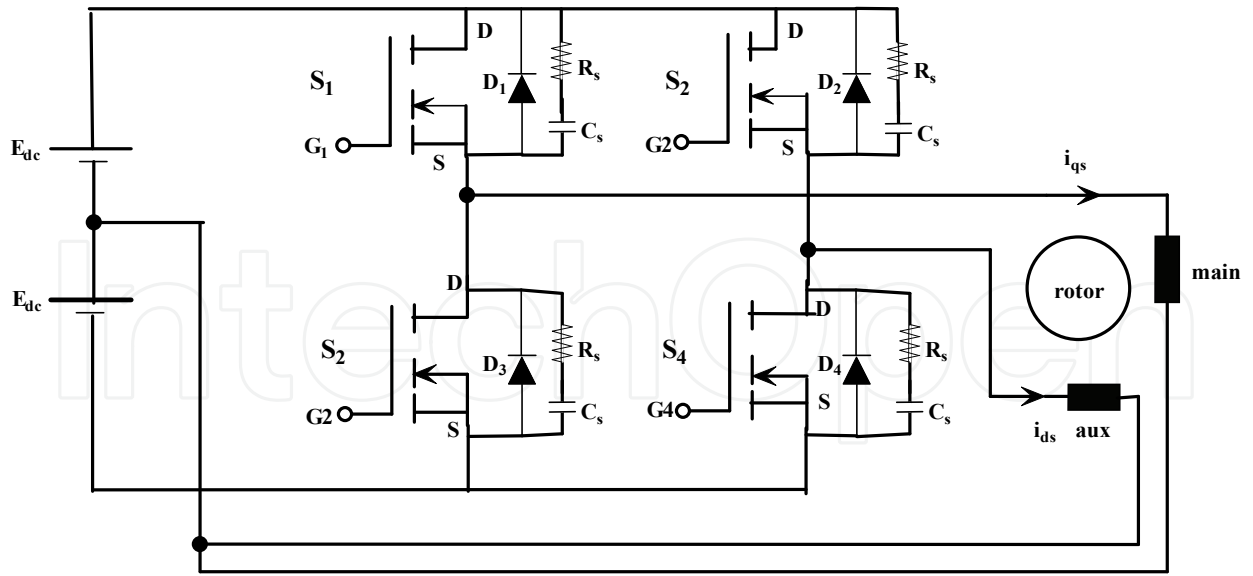
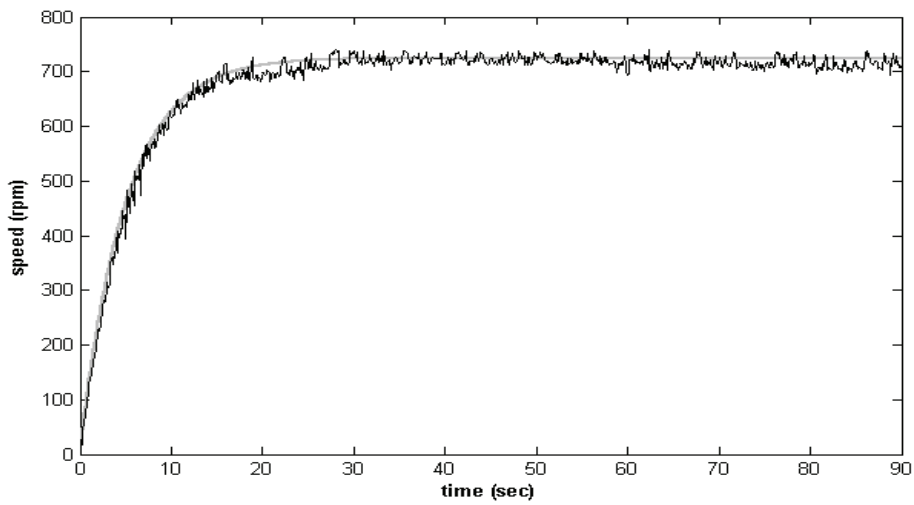
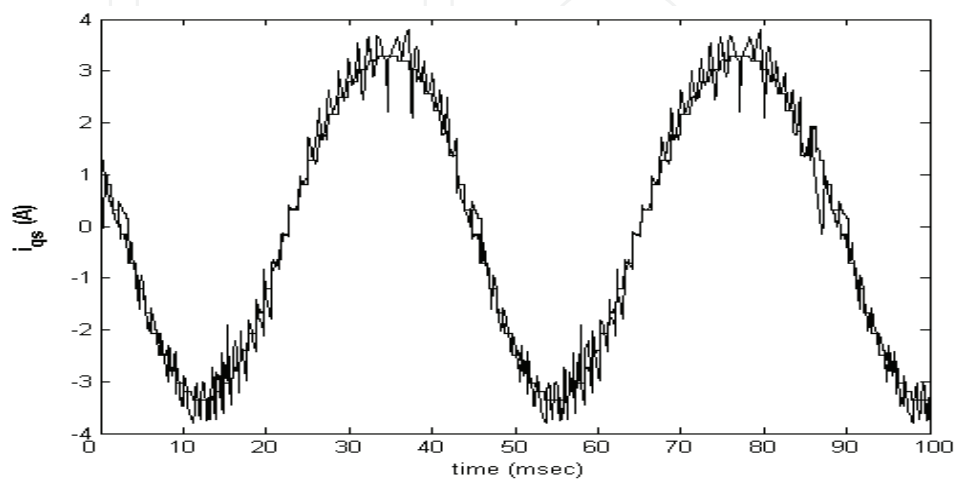


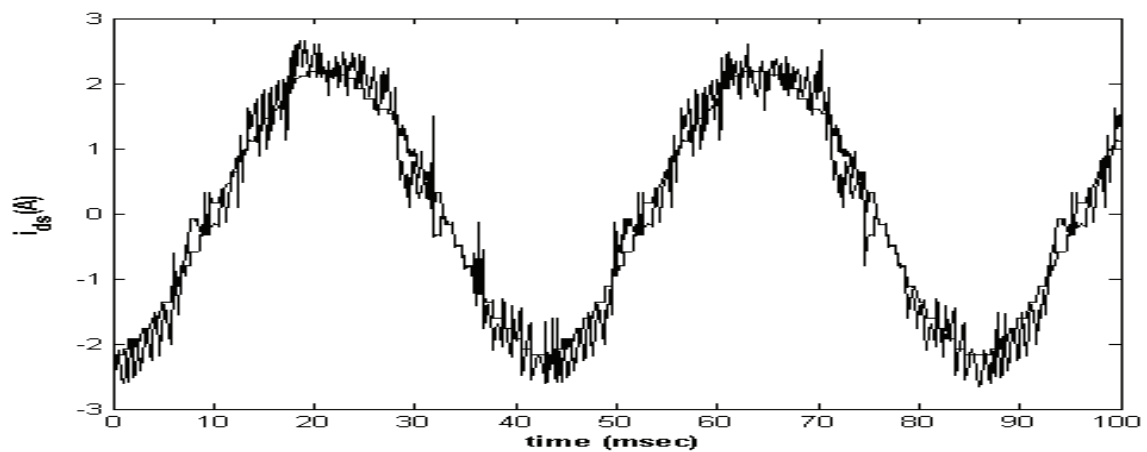
Fig. 9. The power circuit of Four Switch Inverter [FSI]



(a)

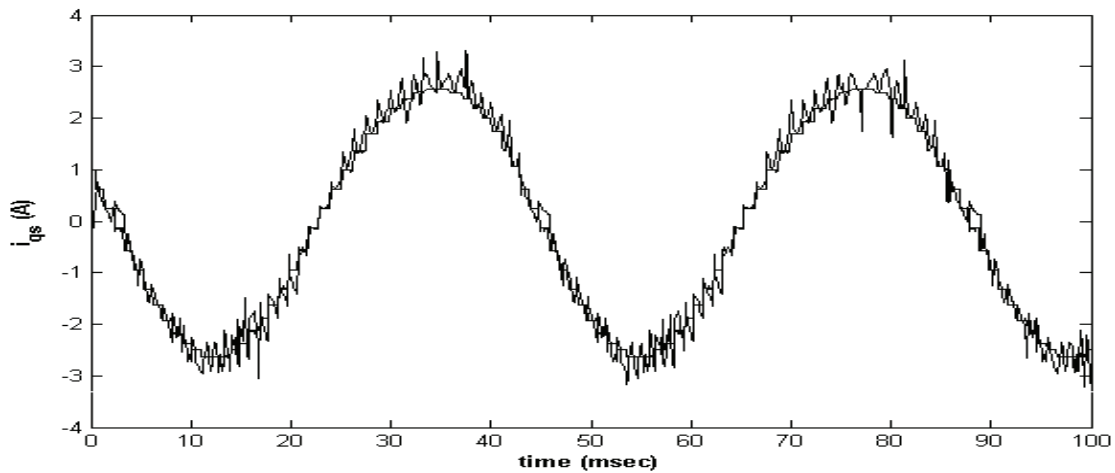


(b)

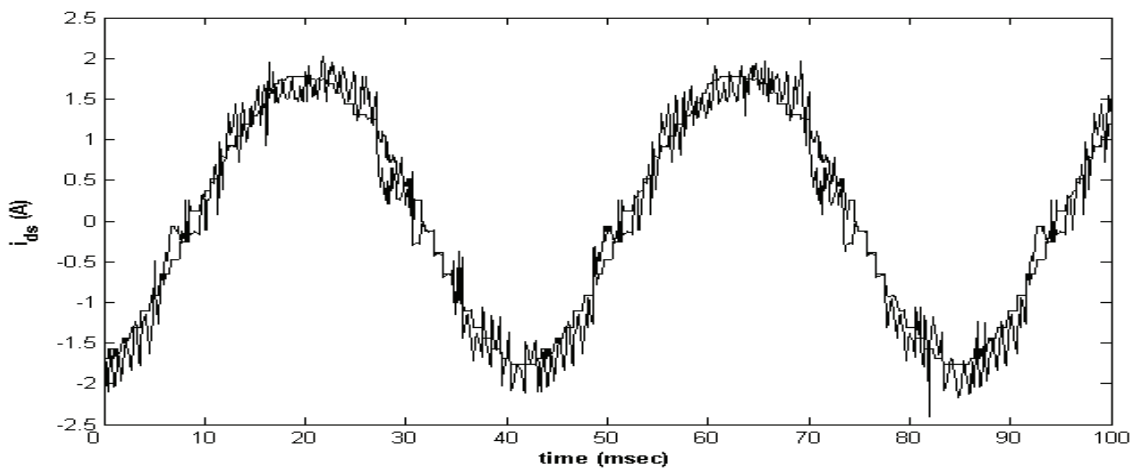


(c)

Fig. 10. Experimental results of FOC method; the reference and actual speed, (b) the reference and actual current in q-axis, (c) The reference and actual current in d-axis



(a)



(b)

Fig. 11. Experimental results of FOC method based on PSO. (a) The reference and actual current in q-axis, the reference and actual current in d-axis

Finally, these results demonstrate that, the FOC based on PSO method saves more energy than conventional FOC method. Thus, the efficiency with PSO is improved than it's at FOC.

3. Maximum efficiency and minimum operating cost of induction motors

This section presents another application of PSO for losses and operating cost minimization control in the induction motor drives. Two control strategies for induction motor speed control are proposed. Those two strategies are based on PSO and called Maximum Efficiency Strategy and Minimum Operating Cost Strategy [A. Hamid et al. 2006]. The proposed technique is based on the principle that the flux level in the machine can be adjusted to give the minimum amount of losses and minimum operating cost for a given value of speed and load torque. The main advantages of the proposed technique are; its simple structure. It is a straightforward maximization of induction motor efficiency and its operating cost for a given load torque. As was demonstrated, PSO is efficient in finding the optimum operating machine's flux level. The optimum flux level is a function of the machine operating point.

The main induction motor losses are usually split into five components: stator copper losses, rotor copper losses, iron losses, mechanical losses, and stray losses [Kioskeridis & Margaris, 1996].

The efficiency that decreases with increasing losses can be improved by minimizing the losses. Copper losses reduce with decreasing the stator and the rotor currents, while the core losses essentially increase with increasing air-gap flux density. A study of the copper and core losses components reveals that their trends conflict. When the core losses increase, the copper losses tends to decrease. However, for a given load torque, there is an air-gap flux density at which the total losses is minimized. Hence, electrical losses minimization process ultimately comes down to the selection of the appropriate air-gap flux density of operation. Since the air-gap flux density must be variable when the load is changing, control schemes in which the (rotor, air-gap) flux linkage is constant will yield sub-optimal efficiency operation especially when the load is light. Then to improve the motor efficiency, the flux must be reduced when it operates under light load conditions by obtaining a balance between copper and iron losses.

The challenge to engineers, however, is to be able to predict the appropriate flux values at any operating points over the complete torque and speed range which will minimize the machines losses, hence maximizing the efficiency. In general, there are three different approaches to improve the induction motor efficiency especially under light-load.

a. Losses Model Controller (LMC)

This controller depends on a motor losses model to compute the optimum flux analytically. The main advantage of this approach is its simplicity and it does not require extra hardware. In addition, it provides smooth and fast adaptation of the flux, and may offer optimal performance during transient operation. However, the main problem of this approach is that it requires the exact values of machine parameters. These parameters include the core losses and the main inductance flux saturation, which are unknown to the users and change considerably with temperature, saturation, and skin effect. In addition, these parameters may vary due to changes in the operating conditions. However, with continuing improvement of evolutionary parameter determination algorithms, the disadvantages of motor parameters dependency are slowly disappearing.

b. Search Controller (SC)

This controller measures the input power of the machine drive regularly at fixed time intervals and searches for the flux value, which results in minimum power input for given

values of speed and load torque. This particular method does not demand knowledge of the machine parameters and the search procedure is simple to implement.

However, some disadvantages appear in practice, such as continuous disturbances in the torque, slow adaptation (7sec.), difficulties in tuning the algorithm for a given application, and the need for precise load information. In addition, the precision of the measurements may be poor due to signal noise and disturbances. This in turn may cause the SC method to give undesirable control performance. Moreover, nominal flux is applied in transient state and is tuned after the system reaches steady state to an optimal value by numerous increments, thus lengthening the optimization process. Therefore, the SC technique may be slow in obtaining the optimal point. In addition, in real systems, it may not reach a steady state and so cause oscillations in the air gap flux that result in undesirable torque disturbances. For these reasons, this is not a good method in industrial drives.

c. Look Up Table Scheme

It gives the optimal flux level at different operating points. This table, however, requires costly and time-consuming prior measurements for each motor. In this section, a new control strategy uses the loss model controller based on PSO is proposed. This strategy is simple in structure and has the straightforward goal of maximizing the efficiency for a given load torque. The resulting induction motor efficiency is reasonably close to optimal. It is well known that the presence of uncertainties, the rotor resistance, for instance makes the result no more optimal. Digital computer simulation results are obtained to demonstrate the effectiveness of the proposed method.

3.1 Definition of operating strategies

The following definitions are useful in subsequent analyses. Referring to the analysis of the induction motor presented in [A. Hamid et al. 2006], the per-unit frequency is

$$a = \frac{\omega_e}{\omega_b} = \frac{\omega_s + \omega_r}{\omega_b} \quad (39)$$

The slip is defined by

$$s = \frac{\omega_s}{\omega_b} = \frac{\omega_s}{\omega_s + \omega_r} \quad (40)$$

The rotor current is given by

$$I_r' = \frac{\phi_m}{\sqrt{\left(\frac{r_r'}{sa}\right)^2 + X_{lr}'^2}} \quad (41)$$

The electromagnetic torque is given by

$$T_e = \frac{\left(\frac{r_r'}{sa}\right)}{\left(\frac{r_r'}{sa}\right)^2 + X_{lr}'^2} \phi_m^2 \quad (42)$$

The stator current is related to the air gap flux and the electromagnetic torque as:

$$I_s = \sqrt{\left(S_1 \phi_m + S_2 \phi_m^3 + S_3 \phi_m^5\right)^2 + C_L \frac{T_e^2}{\phi_m^2}} \quad (43)$$

Where

$$C_L = 1 + 2 \times \frac{x_{lr}}{x_m}$$

The air gap flux is related to the electromagnetic torque as:

$$\phi_m = \sqrt{\frac{sa}{r_r} \sqrt{\left(\frac{r_r}{sa}\right)^2 + x_{lr}^2} \sqrt{T_e}} \quad (44)$$

The efficiency is defined as the output power divided by the electric power supplied to the stator (inverter losses are included):

$$\text{Efficiency } (\eta) = \frac{P_{out}}{P_{in}} \quad (45)$$

3.1.1 Maximum efficiency strategy

In MES (Maximum Efficiency Strategy), the slip frequency is adjusted so that the efficiency of the induction motor drive system is maximized [A. Hamid et al. 2006].

The induction motor losses are the following:

1. Copper losses: these are due to flow of the electric current through the stator and rotor windings and are given by:

$$P_{cu} = r_s I_s^2 + r_r I_r^2 \quad (46)$$

2. Iron losses: these are the losses due to eddy current and hysteresis, given by

$$P_{core} = K_e (1 + S^2) a^2 \phi_m^2 + K_h (1 + S) a \phi_m^2 \quad (47)$$

3. Stray losses: these arise on the copper and iron of the motor and are given by:

$$P_{cu} = C_{str} \omega_r^2 I_r^2 \quad (48)$$

4. Mechanical losses: these are due to the friction of the machine rotor with the bearings and are given by:

$$P_{fw} = C_{fw} + \omega_r^2 \quad (49)$$

5. Inverter losses: The approximate inverter loss as a function of stator current is given by:

$$P_{inv} = K_{1inv} i_s^2 + K_{2inv} i_s \quad (50)$$

Where: K_{1inv} , K_{2inv} are coefficients determined by the electrical characteristics of a switching element where: $K_{1inv} = 3.1307e-005$, $K_{2inv} = 0.0250$.

The total power losses are expressed by:

$$P_{losses} = P_{cu} + P_{core} + P_s + P_{fw} + P_{inv} = \left[r_s I_s^2 + r_r' I_r'^2 \right] + \left[K_e (1 + S^2) a^2 \phi_m^2 \right] + \left[K_h (1 + S) a \phi_m^2 \right] + \left[C_{str} \omega_r^2 I_r'^2 \right] + \left[K_{1inv} i_s^2 + K_{2inv} i_s \right] \quad (51)$$

The output power is given by:

$$P_{out} = T_L \times \omega_r \quad (52)$$

The input power is given by:

$$P_{in} = P_{out} + P_{losses} = P_{cu} + P_{core} + P_s + P_{fw} + P_{inv} = \left[r_s I_s^2 + r_r' I_r'^2 \right] + \left[K_e (1 + S^2) a^2 \phi_m^2 \right] + \left[K_h (1 + S) a \phi_m^2 \right] + \left[C_{str} \omega_r^2 I_r'^2 \right] + \left[K_{1inv} i_s^2 + K_{2inv} i_s \right] + T_L \times \omega_r \quad (53)$$

The efficiency is expressed as:

$$\eta = \frac{T_L \times \omega_r}{\left[r_s I_s^2 + r_r' I_r'^2 \right] + \left[K_e (1 + S^2) a^2 \phi_m^2 \right] + \left[K_h (1 + S) a \phi_m^2 \right] + \left[C_{str} \omega_r^2 I_r'^2 \right] + \left[K_{1inv} i_s^2 + K_{2inv} i_s \right] + T_L \times \omega_r} \quad (54)$$

The efficiency maximization of the induction motor problem can be formulated as follows:

$$\text{Maximize } \eta (T_L, \omega_s, \omega_r) \quad (55)$$

The maximization should observe the fact that the amplitude of the stator current and flux cannot exceed their specified maximum point.

3.1.2 Minimum operating cost strategy

In Minimum Operating cost Strategy (MOCS), the slip frequency is adjusted so that the operating cost of the induction motor is minimized. The operating cost of the induction machine should be calculated over the whole life cycle of the machine. That calculation can be made to evaluate the cost of the consumed electrical energy. The value of average energy cost considering the power factor penalties can be determined by the following stages [A. Hamid et al. 2006]:

1. If $0 \leq \text{PF} < 0.7$

$$C = C_0 \left[1 + \left(\frac{0.9 - PF}{0.01} \right) \times \frac{1}{100} \right] \quad (56)$$

2. If $0.7 \leq PF \leq 0.92$, If $PF \geq 0.9$, $PF = 0.9$

$$C = C_0 \left[1 + \left(\frac{0.9 - PF}{0.01} \right) \times \frac{0.5}{100} \right] \quad (57)$$

3. If $0.9 \leq PF \leq 1$, If $0.95 \leq PF \leq 1$, $PF = 0.95$

$$C = C_0 \left[1 + \left(\frac{0.9 - PF}{0.01} \right) \times \frac{0.7}{100} \right] \quad (58)$$

If the average energy cost C is calculated, it can be used to establish the present value of losses. The total cost of the machine is the sum of its initial cost plus the present worth value of losses and maintenance costs.

$$PW_L = C \times T \times N \times P_{out} \times \left[\frac{1}{\eta} - 1 \right] \quad (59)$$

Where:

PW_L = present worth value of losses

C_0 = energy cost per kWh,

C = modified energy cost per kWh

T = running time per year (Hrs / year)

N = evaluation life (years)

P_{out} = the output power (kW)

η = the efficiency

The operating cost minimization of the induction motor problem can be formulated as follows:

$$\text{Minimize } PW_L(T_L, \omega_s, \omega_r) \quad (60)$$

3.2 Simulation results

The simulation is carried out on a three-phase, 380 V, 1-HP, 50 Hz, and 4-pole, squirrel cage induction motor. The motor parameters are $R_s=0.0598$, $X_{ls}=0.0364$, $X_m=0.8564$, $X_{lr}=0.0546$, $R_r=0.0403$, $K_e=0.0380$, $K_h=0.0380$, $C_{str}=0.0150$, $C_{fw}=0.0093$, $S_1=1.07$, $S_2=-0.69$, $S_3=0.77$. For cost analysis, the following values were assumed: $C_0=0.05$, $N=15$, $T=8000$. The task of PSO controller is to find that value of slip at which the maximum efficiency occurs. At certain load torque and rotor speed, the PSO controller determines the slip frequency ω_s at which the maximum efficiency and minimum operating cost occur. The block diagram of the optimization process based on PSO is shown in Fig.12. To observe the improvements in efficiency using the suggested PSO controller, Fig. 13 shows the efficiency of the selected machine for all operating conditions using conventional methods (constant voltage to frequency ratio, field oriented control strategy) and using the proposed PSO controller at different rotor speed levels, $W_r = 0.2$ PU, and $W_r = 1$ PU respectively [A. Hamid et al. 2006]. This figure shows that a considerable energy saving is achieved in comparison with the conventional method (field oriented control strategy and constant voltage to frequency

ratio) especially at light loads and small rotor speed. Figure 14 compares the efficiency of the induction motor drive system under the maximum efficiency strategy with the minimum operating cost strategy at $W_r = 1$ PU. It is obvious from the figure that the efficiency is almost the same for both strategies for all operating points.

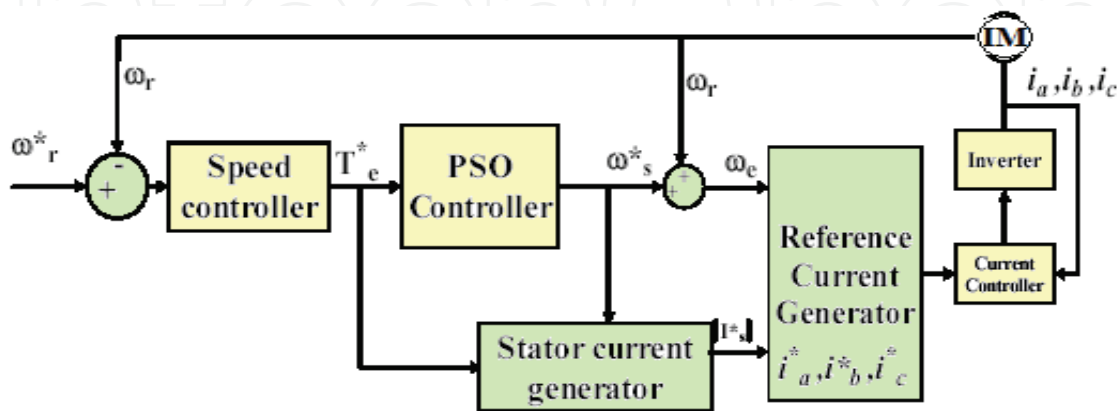
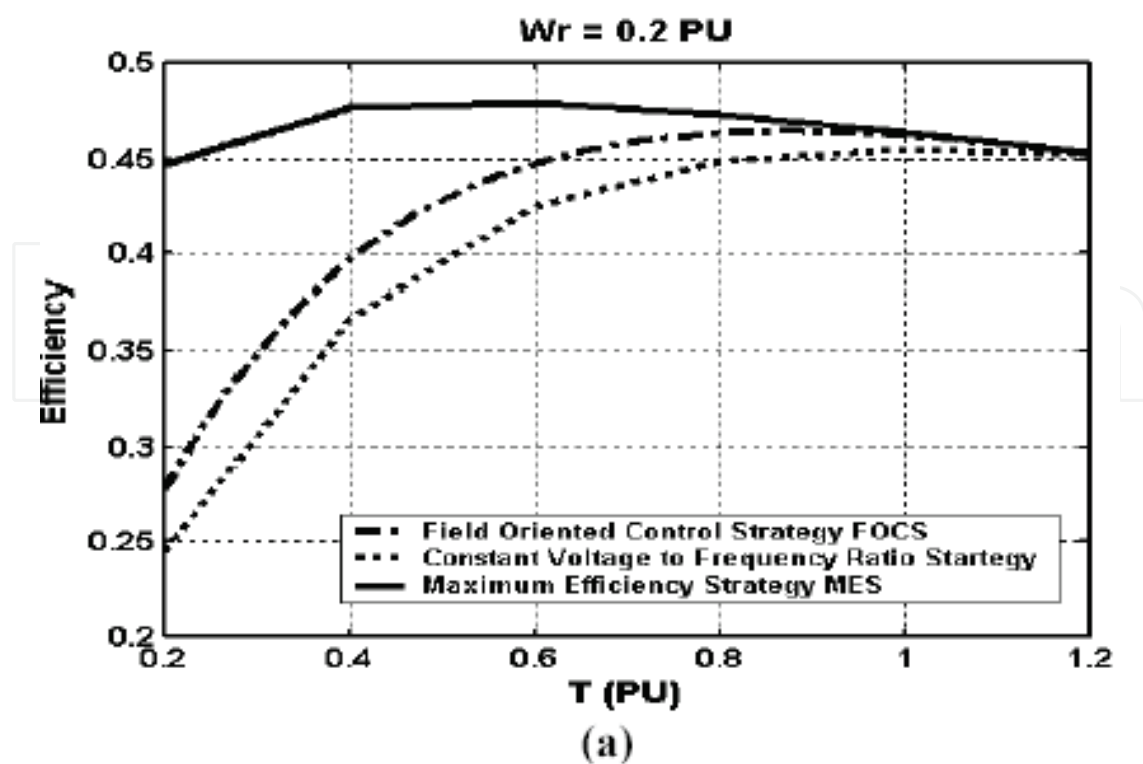


Fig. 12. The proposed drive system based on PSO controller



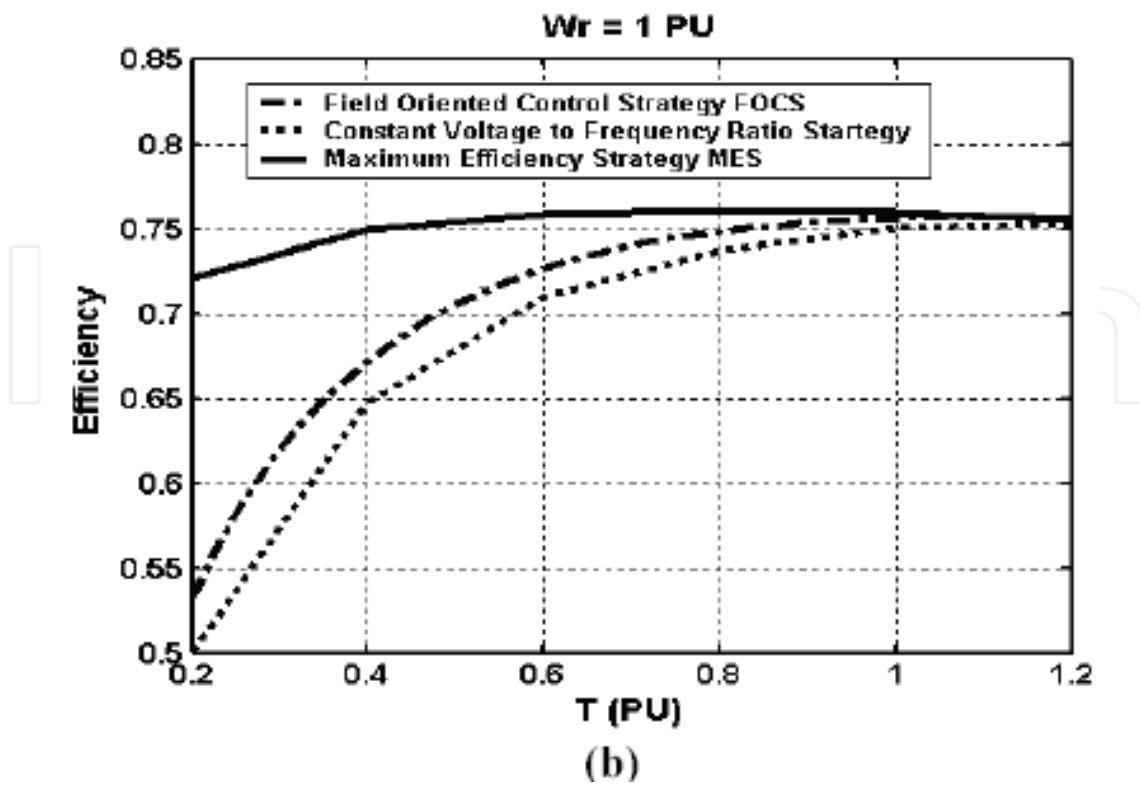


Fig. 13. The efficiency of the induction motor using the maximum efficiency strategy compared with the efficiency using the conventional methods at (a) $W_r = 0.2$ PU, (b) $W_r = 1$ PU [A. Hamid et al. 2006].

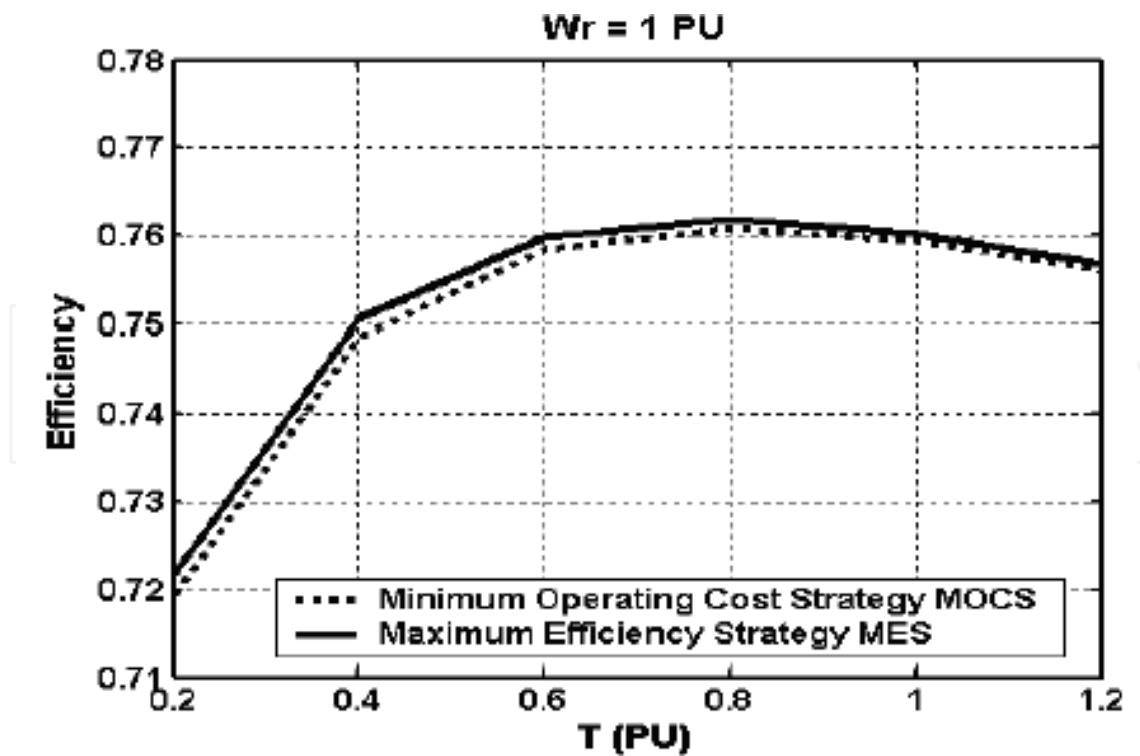


Fig. 14. The efficiency of the induction motor using the maximum efficiency strategy compared with the efficiency using minimum operating cost strategy at $W_r = 1$ PU

Table 5 shows the efficiency comparison using few examples of operating points. Figure 15 compares the power factor of the induction motor drive system under the maximum efficiency strategy with the minimum operating cost strategy at $W_r = 1$ PU. Finally, the proposed PSO-controller adaptively adjusts the slip frequency such that the drive system is operated at the minimum loss and minimum operating cost. It was found that the optimal system slip changes with variations in speed and load torque. When comparing the proposed strategy with the conventional methods field oriented control strategy and constant voltage to frequency ratio). It was found that a significant efficiency improvement especially at light loads for all speeds. On the other hand, small efficiency improvement is achieved at near rated loads (see Fig.13, and Fig.15).

Efficiency comparison for $\omega_r = 1$ PU				
T (PU)	Constant voltage to frequency ratio	Field oriented control	Maximum efficiency strategy	Minimum Operating Cost Strategy
0.2	0.5003	0.5330	0.7217	0.7193
0.4	0.6482	0.6730	0.7506	0.7485
0.6	0.7100	0.7271	0.7598	0.7584
0.8	0.7384	0.7494	0.7618	0.7608
1	0.7508	0.7569	0.7603	0.7595
1.2	0.7544	0.7566	0.7568	0.7562

Table 5. Some examples of efficiency comparison under different Load torque levels and $W_r = 1$ PU [A. Hamid et al. 2006].

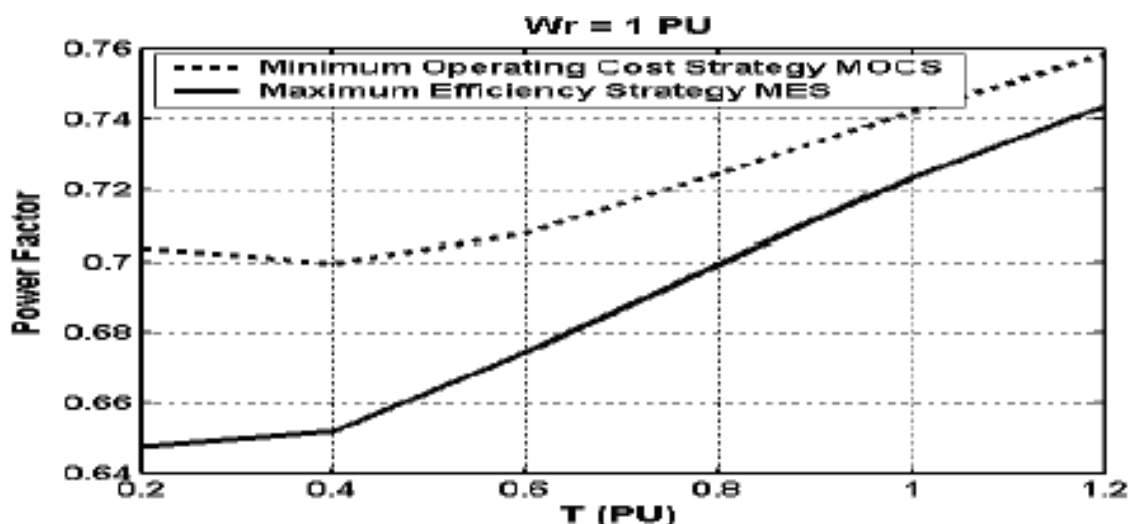


Fig. 15. The power factor of the induction motor using the maximum efficiency strategy compared with the efficiency using minimum operating cost strategy at $W_r = 1$ PU [A. Hamid et al. 2006]

4. Optimal electric drive system for fuel cell hybrid electric vehicles

Although there are various FC technologies available for use in vehicular systems, the proton exchange membrane FC (PEMFC) has been found to be a prime candidate, since

PEMFC has higher power density and lower operating temperatures when compared to the other types of FC systems. A stand-alone FC system integrated into an automotive powertrain is not always sufficient to satisfy the load demands of a vehicle. Although FC systems exhibit good power capability during steady-state operation, the response of fuel cells during transient and instantaneous peak power demands is relatively poor. Thus, the FC system can be hybridized with supercapacitors (SC) or batteries to meet the total power demand of a hybrid electric vehicle (HEV) [Van Mierlo et. al, 2006; Paladini et. al, 2007].

In this section, a new control strategy based PSO algorithm is proposed for the Fuel Cell/Supercapacitor hybrid electric vehicles to optimize the electric drive system [Hegazy & Van Mierlo, 2010]. Many factors influence on the performance of the electric drive system. These factors are mass, volume, size, efficiency, fuel consumption and control strategy. Therefore, the PSO is proposed to minimize the cost, the size and the mass of the powertrain sources (Fuel cell, and supercapacitor) as well as minimum fuel consumption and improves the efficiency of the system. PSO algorithm searches for global optimization for nonlinear problems with multi-objective. For a given driving cycle, the size and the cost of fuel cell and supercapacitor are minimized by identifying the best number of units of each, respectively. Three methods have been designed to achieve the optimal sizing. These are conventional method, trial and error, as was mentioned in [Wu & Gao, 2006], GA, and PSO. In addition, the hydrogen consumption is minimized by the evaluation of the optimal power distribution between fuel cell (main source) and supercapacitor (auxiliary source). Three control strategies are implemented to minimize the hydrogen consumption and maintain the state of charge (SOC) of the supercapacitor ($SOC_{initial} = SOC_{final}$), which are control strategy based on Efficiency Map (CSEM), Control strategy based on PSO (CSPSO), and control strategy based on GA (CSGA).

4.1 System description

The power system configuration is illustrated in Fig.16. A hybrid fuel cell/supercapacitor vehicle utilizes a PEM fuel cell as the main power source and a supercapacitor as the auxiliary power source. A multiple-input power electronic converter (MIPEC) is proposed to interface the traction drive requirements. In the MIPEC, the FC is connected to DC Bus

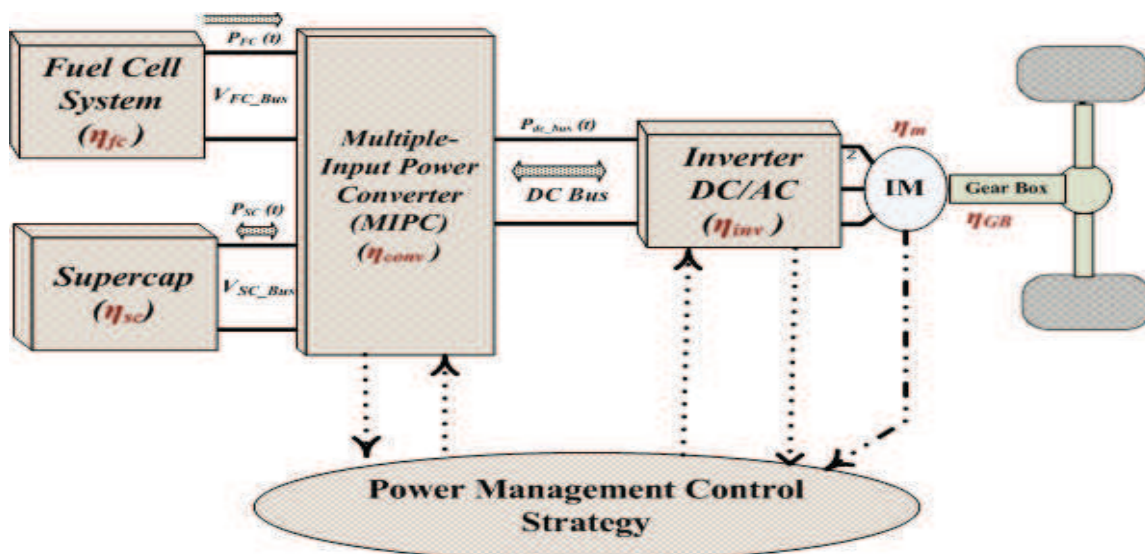


Fig. 16. The drive system of the Fuel Cell/Supercapacitor Hybrid Electric Vehicle

via a Boost DC/DC converter ($\eta_B = \eta_{conv}$) and the supercapacitor is connected to DC Bus via a Buck/Boost converter ($\eta_{B/B} = \eta_{conv}$). The desired value of the DC-Bus voltage is chosen to be 400 V with variations of $\pm 10\%$ are permissible. The power supplied by the powertrain has to be obtaining from the power demand predicted by the dynamics of the vehicle. The efficiency of each component in the hybrid powertrain is taken into account. A detailed model of the powertrain is built in MATLAB /SIMULINK.

4.1.1 Modeling of the vehicle power demand

The load force of the vehicle consists of gravitational force, rolling resistance, aerodynamic drag force, and acceleration force. Hereby, the load power required for vehicle acceleration can be written as [Hegazy & Van Mierlo, 2010; Hegazy et. al 2010]

$$P_{load} = \frac{(F_g + F_{roll} + F_{AD} + F_{acc}) * V}{\eta_{GB}} \quad (61)$$

$$F_g = M \cdot g \cdot \sin(\alpha) \quad (62)$$

$$F_{roll} = M \cdot g \cdot f_r \cdot \cos(\alpha) \quad (63)$$

$$F_{AD} = 0.5 \rho_a \cdot C_D \cdot A_F \cdot V^2 \quad (64)$$

$$F_{acc} = M \cdot \frac{dV}{dt} \quad (65)$$

$$V = \omega_w \cdot r_w \quad (66)$$

The total electric power required from sources can be expressed as:

$$P_{req} = \frac{P_{load}}{\eta_m \cdot \eta_{Inv} \cdot \eta_{Conv}} \quad (67)$$

The parameters of the vehicle are given in Table 6. The analysis of FCHEV is performed with two standard driving cycles:

1. The Federal Test Procedure (FTP75) Urban;
2. The New European Driving Cycle (NEDC)

Suppose that the efficiencies of the motor (η_m), inverter (η_{Inv}), and MIPEC ($\eta_{Conv} = \eta_B = \eta_{B/B}$) are 0.90, 0.94 and 0.95, respectively.

M	Vehicle mass (kg)	1450	A_f	Front Area (m2)	2.13
f_r	Rolling Resistance Coefficient	0.013	r_w	Radius of the wheel (m)	0.28
C_D	Aerodynamic Drag Coefficient (CD)	0.29	ρ_a	Air density (kg/m3)	1.202

Table 6. Vehicle Parameters [Wu & Gao, 2006]

4.2 Optimal powertrain design

The first goal of optimization algorithm, PSO, is to minimize the cost, the mass, and the volume of the fuel cell (FC) and supercapacitor (SC). It is assumed that, the cost, the mass and the volume of the fuel cell and supercapacitor are a function of the number of the parallel units N_{fcp} and N_{scp} , respectively. The multi-objective criterion should be aggregated in a single objective function if the design objective is to embody a unique solution. The objective function can be formulated as follows:

$$F(x) = w_1 \text{cost} + w_2 \text{mass} + w_3 \text{volume} \quad (68)$$

$$\text{cost} = C1. N_{fcs}. N_{fcp} + C2. N_{scs}. N_{scp} \quad (69)$$

The coefficients of the terms in $F(x)$ were chosen to reflect the importance of minimizing the cost, the mass and the volume. Suppose that w_1 , w_2 , and w_3 are 0.35, 0.35, and 0.3, respectively. Figure 17 presents the flowchart of the execution of PSO, which evaluates the optimal number of the FC units and the supercapacitor units by using MATLAB /SIMULINK. The layout of the fuel-cell stack and layout of the supercapacitor system are shown in Fig.18 (a) and (b), respectively. The constraints of the optimization problems are mentioned in [Hegazy & Van Mierlo, 2010].

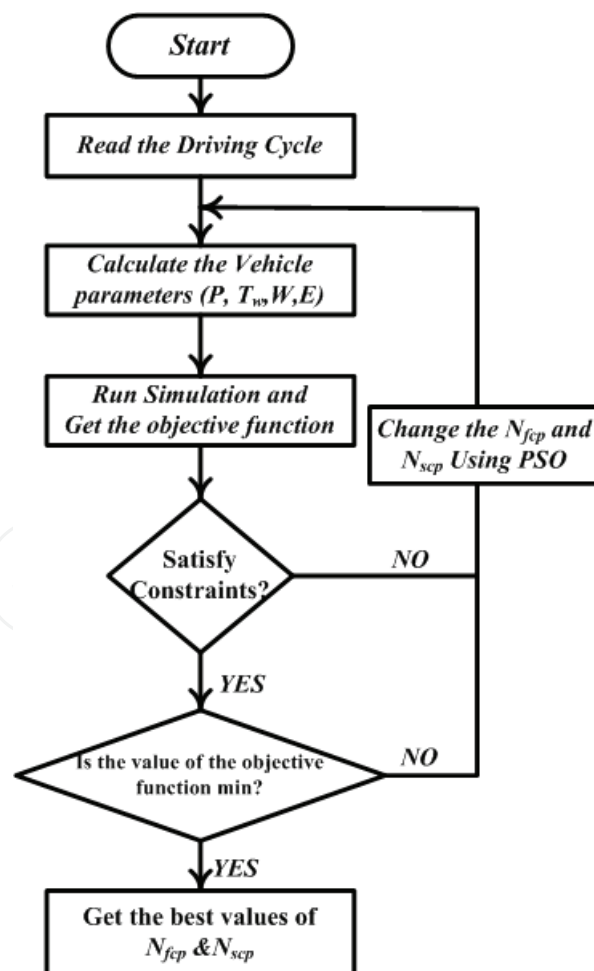
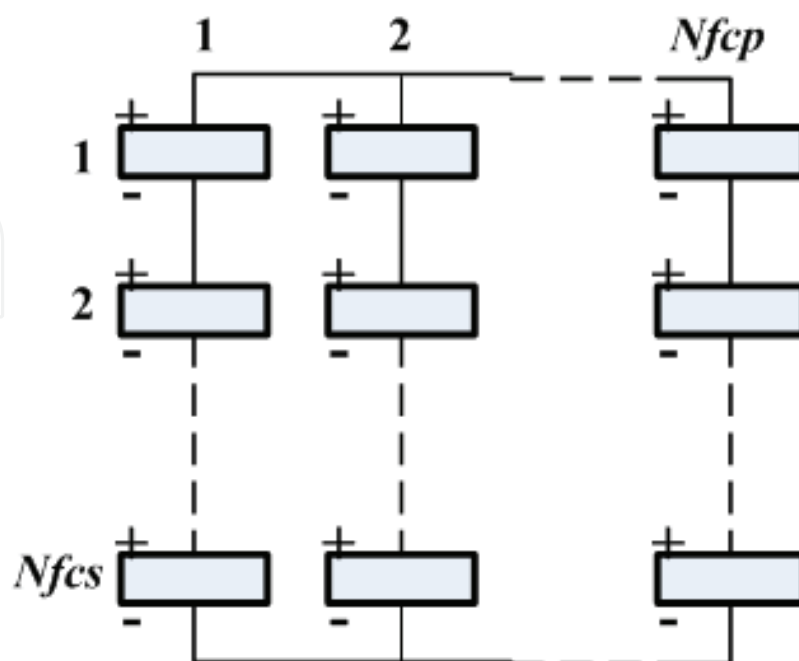
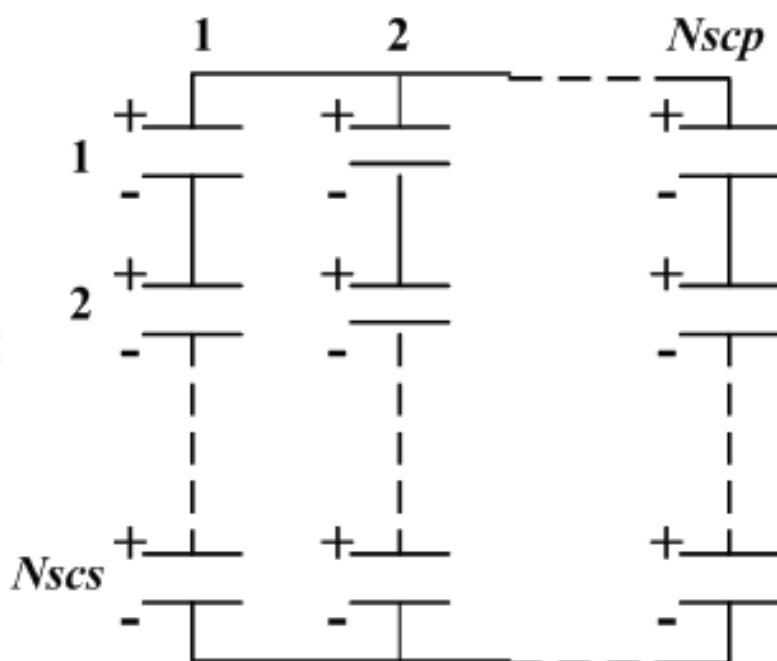


Fig. 17. The flowchart of the execution of PSO [Hegazy et. al 2010]



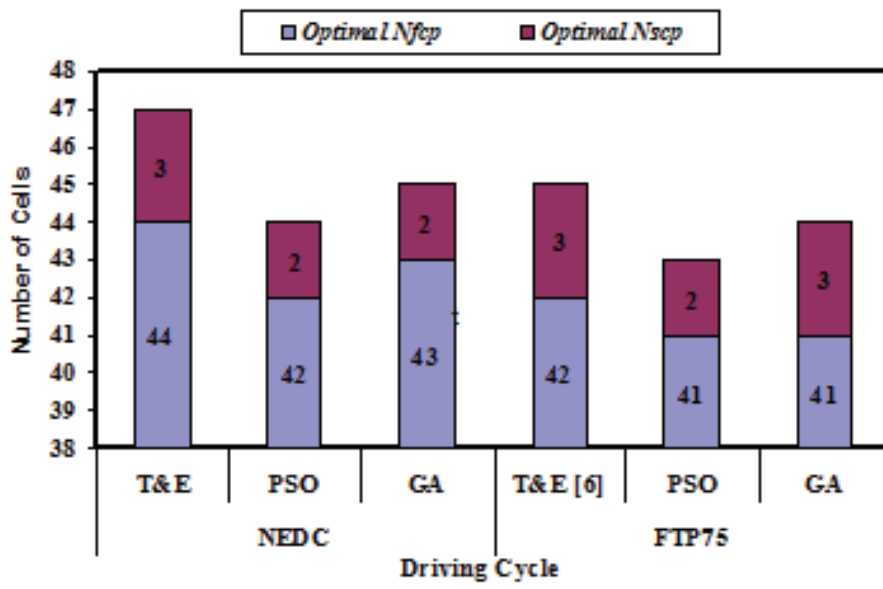
(a)



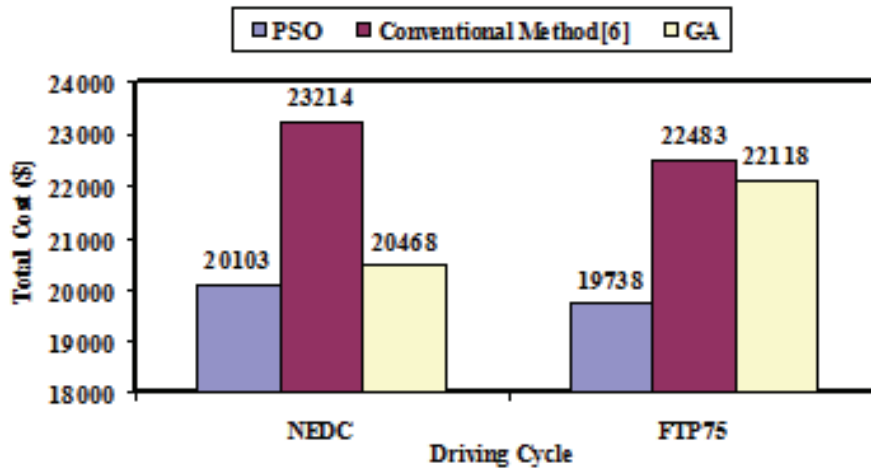
(b)

Fig. 18. (a) Layout of the FC; (b) Layout of the SC

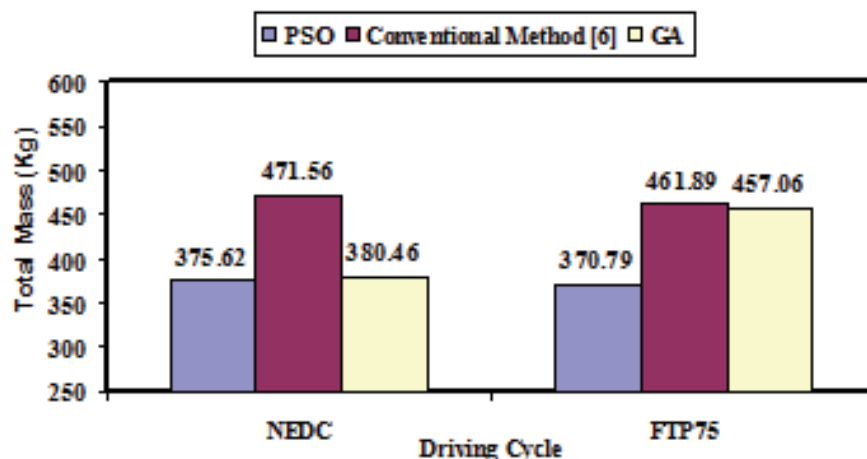
Based on minimizing the objective function $F(x)$ in (68), the results of the optimal design and components sizing of the FC/SC powertrain are shown in Fig.19. The analyses and parameters of the FC and the SC are mentioned in [Hegazy & Van Mierlo, 2010].



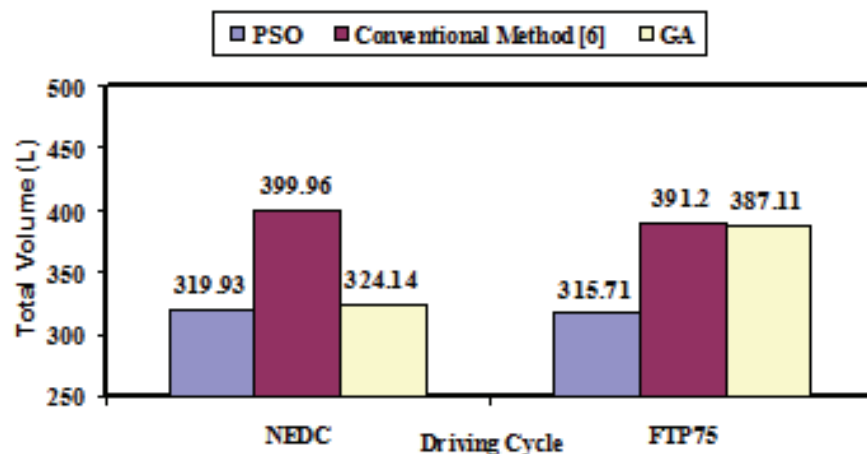
(a) The optimal numbers of cells of FC and SC



(b) The cost of the FC/SC components



(c) The mass of the FC/SC components



(d) The mass of the FC/SC components

Fig. 19. The Comparative of the optimal design between different methods for FC/SC HEV

4.3 Optimal Power Control (OPC)

The second goal of the PSO is to minimize the vehicle fuel, hydrogen, consumption while maintaining the supercapacitor state of charge. As a hybrid powertrain is under consideration, a power management strategy is required to define what both the FC and SC powers are. The global optimization algorithms, such as GA and dynamic programming (DP), achieve an optimal power control for FC/SC hybrid electric vehicle, which leads to the lowest hydrogen consumption and maintains the supercapacitor SOC [Sinoquet et. al 2009; Sundstrom & Stefanopoulou 2006].

In this study, the optimal power control can be achieved by using PSO and GA for a given driving cycle. Suppose that the degree of hybridization of the fuel cell is K_{fc} at time t and K_{soc} , Proportional controller gain, which used to adapt the SOC during charging from the FC. A balance equation can naturally be established, since the sum of power from both sources has to be equal to the required power at all times:

$$P_{req}(t) = P_{fc}(t) + P_{sc}(t) \quad (70)$$

$$K_{fc}(t) = \frac{P_{fc}(t)}{P_{req}(t)} \quad (71)$$

The net energy consumed from the FC at time t can be computed as follows:

$$E_{fc}(t) = \int_0^t \frac{P_{fc}(t)}{\eta(P_{fc}(t))} dt \quad (72)$$

The cost function can be expressed as follows:

$$F_2(x) = \frac{1}{Elow} \sum_{K=0}^N \frac{P_{fc_{Opti}}(k)}{\eta(P_{fc_{Opti}}(k))} \Delta T \quad (73)$$

The Optimal fuel cell power output, $P_{fc_{Opti}}$, is calculated based on the SOC of the supercapacitor and power demand, P_{req} , as follows:

$$P_{fc_{Opti}}(k) = K_{fc}(k) P_{req}(k) + K_{soc}(k) (P_{fc_{max}} - P_{fc_{min}}) \left[\frac{SOC_{ref} - SOC(k)}{(SOC_{max} - SOC_{min})/2} \right] \quad (74)$$

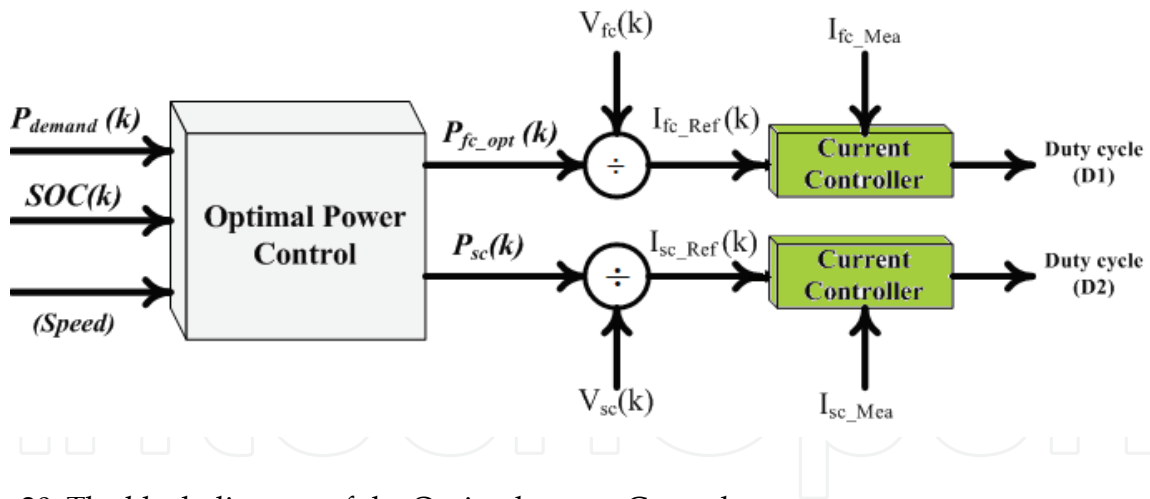
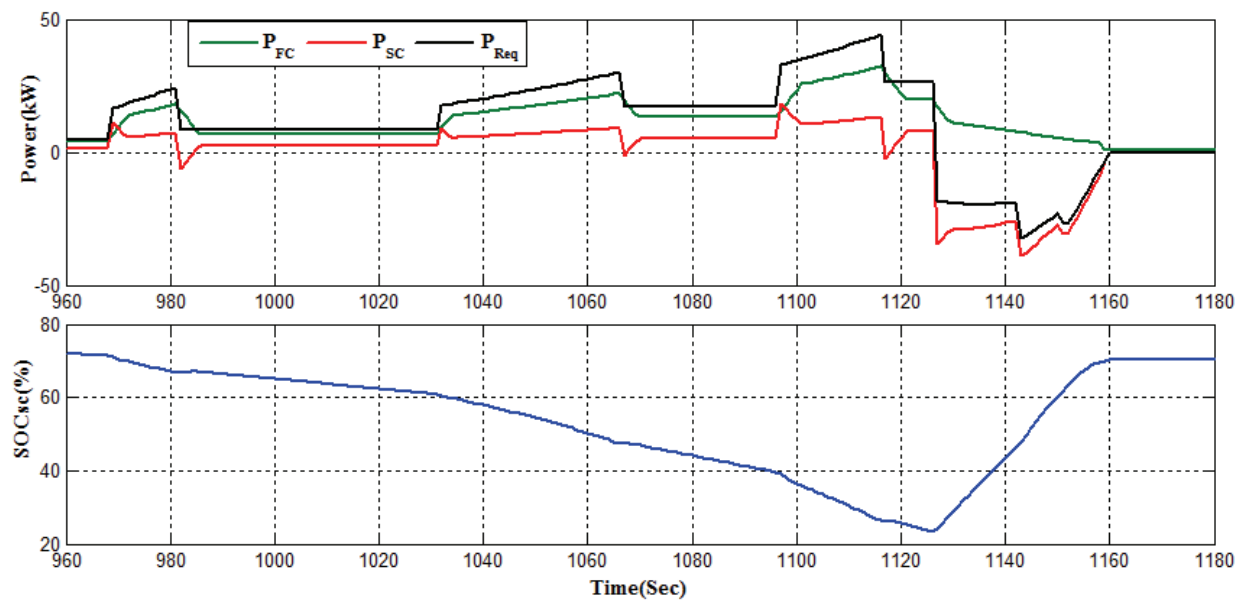


Fig. 20. The block diagram of the Optimal power Control

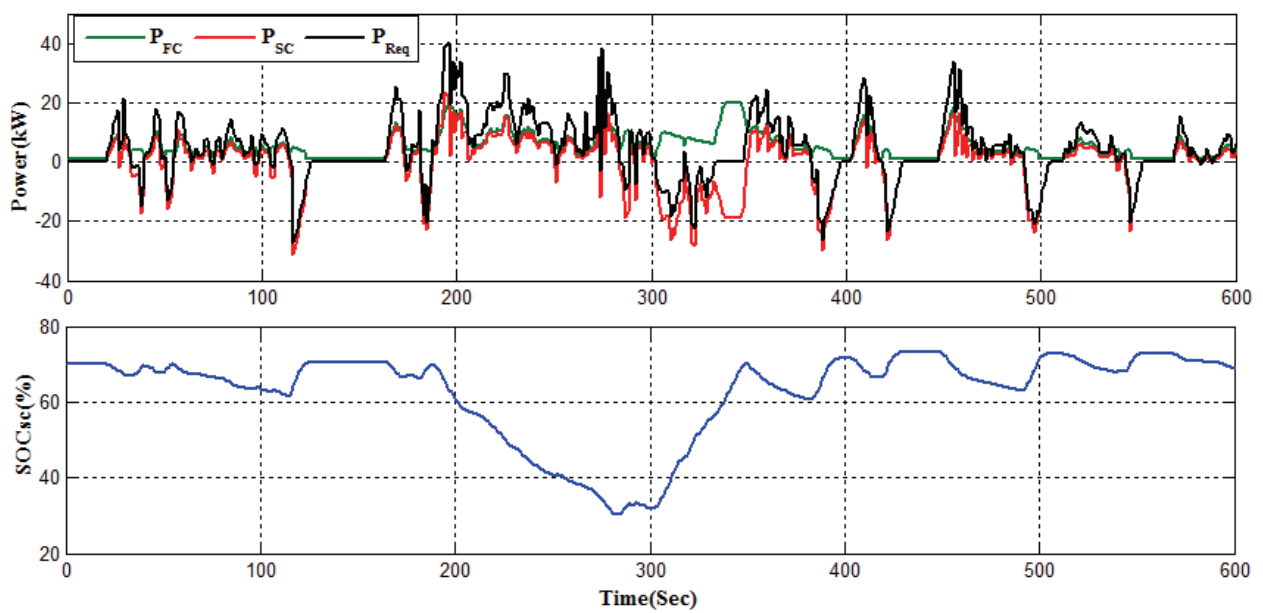
Where: $N = T/\Delta T$ is number of samples during the driving cycle, and $\Delta T = 1s$ is the sampling time.

The block diagram of the optimal power control based on optimization algorithm is shown in Fig.20.

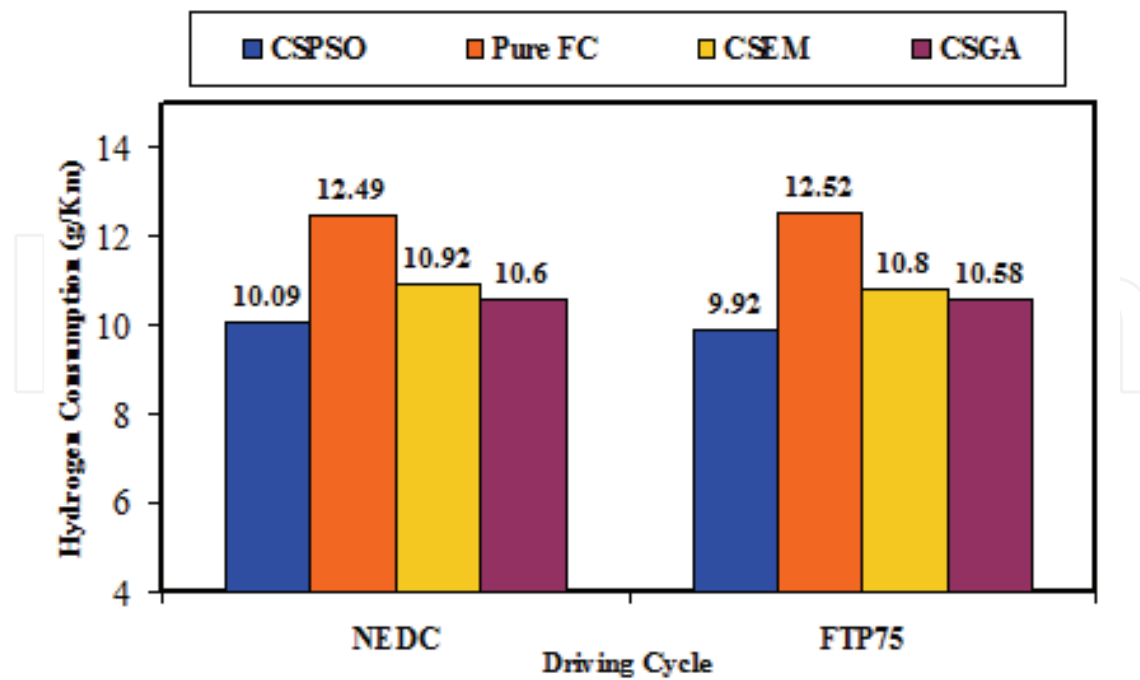
Based on minimizing the objective function $F_2(x)$ in (73), the results of the optimal power sharing based PSO and the comparative study for the FC/SC powertrain are summarized in Fig.21 [Hegazy et. al 2010].



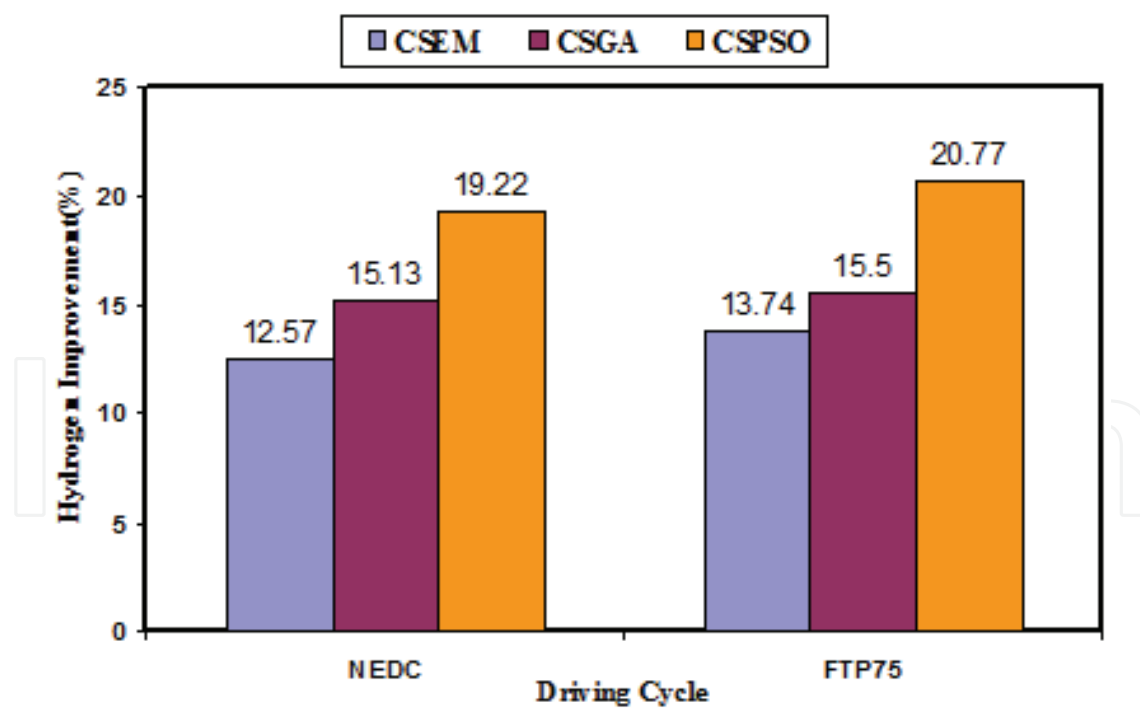
(a) The power sharing between FC and SC on NEDC driving cycle



(b) The power sharing between FC and SC on FTP75 driving cycle



(c) The Comparative of the hydrogen consumption between control strategies



(d) The Hydrogen improvements with respect to pure fuel cell without SC

Fig. 21. The results of the optimal power Control for FC/SC

5. Conclusion

This chapter deals with the applicability of swarm intelligence (SI) in the form of particles swarm optimization (PSO) used to achieve the best performance for the electric machines and electric drives. In addition, by analyzing and comparing the results, it is shown that control strategy based on PSO is more efficient than others control strategies to achieve the optimal performance for fuel cell/supercapacitor hybrid electric vehicles (FCHEV).

It is very important to note that, these applications were achieved without any additional hardware cost, because the PSO is a software scheme. Consequently, PSO has positive promises for a wide range of variable speed drive and hybrid electric vehicles applications.

6. Index I

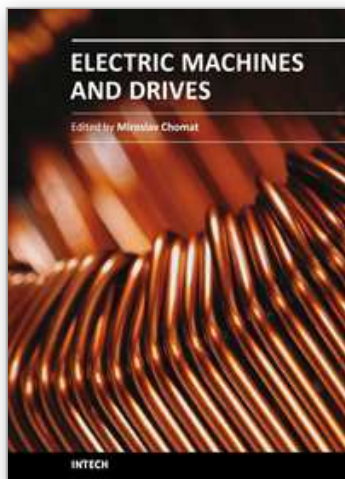
List of principal symbols

ω_e	: synchronous speed
ω_r	: rotor speed
p	: differential operator
r_m, r_a	: main, auxiliary stator windings resistance
r_r	: rotor winding resistance
$R_{feq,d}$: equivalent iron-loss resistance(d and q axis)
L_{lm}, L_{la}	: main, auxiliary stator leakage inductance
L_{md}, L_{mq}	: magnetizing inductance (d& q axis)
L_{lr}	: rotor leakage inductance
K	: turns ratio auxiliary/main windings
T_e	: electromagnetic torque
J	: inertia of motor
$\lambda_{ds,qs}$: stator flux(d and q axis)
$\lambda_{dr,qr}$: rotor flux(d and q axis)
$V_{ds,qs}$: stator voltage (d and q axis)
$i_{ds,qs}$: stator current (d and q axis)
M	: mutual inductance

7. References

- Amin. A. M. A., Korfally. M. I., Sayed. A. A. and Hegazy. O.T. M., (2009), Efficiency Optimization of Two Asymmetrical Windings Induction Motor Based on Swarm Intelligence, IEEE Transactions on Energy Conversion, Vol. 24, No. 1, March 2009
- Amin. A. M. A., Korfally. M. I., Sayed. A. A. and Hegazy. O.T. M., (2006), Losses Minimization of Two Asymmetrical Windings Induction Motor Based on Swarm Intelligence, Proceedings of IEEE- IECON 06 , pp 1150 - 1155, Paris , France , Nov. 2006 .
- Amin. A. M. A., Korfally. M. I., Sayed. A. A. and Hegazy. O.T. M., (2007), Swarm Intelligence-Based Controller of Two-Asymmetrical Windings Induction Motor, accepted for IEEE. EMDC07, pp 953 -958, Turkey, May 2007.
- Eberhart. R, Kennedy. J, (1995), A New Optimizer Using Particles Swarm Theory, *Proc.*

- Sixth International Symposium on Micro Machine and Human Science (Nagoya, Japan), IEEE Service Center, Piscataway, NJ, pp. 39-43,
- A. Hamid Radwan H., Amin Amr. M. A., Ahmed Refaat S., and El-Gammal Adel A. A. ,(2006), "New Technique For Maximum Efficiency And Minimum Operating Cost Of Induction Motors Based On Particle Swarm Optimization (PSO)", Proceedings of IEEE- IECON 06 , pp 1029 – 1034, Paris , France , Nov. 2006.
- Hegazy Omar, (2006), Losses Minimization of Two Asymmetrical Windings Induction Motor Based on Swarm Intelligence, M.Sc., Helwan University, 2006.
- Hegazy Omar, and Van Mierlo Joeri, (2010), Particle Swarm Optimization for Optimal Powertrain Component Sizing and Design of Fuel cell Hybrid Electric Vehicle, 12th International Conference on Optimization of Electrical and Electronic Equipment, IEEE OPTIM 2010
- Hegazy Omar, Van Mierlo Joeri, Verbrugge Bavo and Ellabban Omar, (2010), Optimal Power Sharing and Design Optimization for Fuel Cell/Battery Hybrid Electric Vehicles Based on Swarm Intelligence, The 25th World Battery, Hybrid and Fuel Cell Electric Vehicle Symposium & Exhibition © EVS-25 Shenzhen, China, Nov. 5-9, 2010.
- Kennedy. J and Eberhart .R, (2001), Swarm Intelligence, Morgan Kaufmann Publishers, Inc., San Francisco, CA
- Kioskeridis, I; Margaris, N., (1996), Losses minimization in scalar-controlled induction motor drives with search controllers" Power Electronics, IEEE Transactions, Volume: 11, Issue: 2, March 1996 Pages: 213 – 220
- Popescu. M, Navrapescu. V, (2000) ,A method of Iron Loss and Magnetizing Flux Saturation Modeling in Stationary Frame Reference of Single and Two -Phase Induction Machines", IEE 2000, Conf. power Elec. & Variable Speed Drives, 140-146
- Sundstrom Olle and Stefanopoulou Anna, (2006), Optimal Power Split in Fuel Cell Hybrid Electric Vehicle with different Battery Sizes, Drive Cycles, and Objectives, Proceedings of the 2006 IEEE International Conference on Control Applications Munich, Germany, October 4-6, 2006.
- Van Mierlo Joeri, Cheng Yonghua, Timmermans Jean-Marc and Van den Bossche Peter, (2006), Comparison of Fuel Cell Hybrid Propulsion Topologies with Super-Capacitor, IEEE, EPE-PEMC 2006, Portorož, Slovenia
- Wu Ying, Gao Hongwei, (2006) ,Optimization of Fuel Cell and Supercapacitor for Fuel-Cell Electric Vehicles, IEEE Transactions On Vehicular Technology, Vol. 55, No. 6, November 2006.



Electric Machines and Drives

Edited by Dr. Miroslav Chomat

ISBN 978-953-307-548-8

Hard cover, 262 pages

Publisher InTech

Published online 28, February, 2011

Published in print edition February, 2011

The subject of this book is an important and diverse field of electric machines and drives. The twelve chapters of the book written by renowned authors, both academics and practitioners, cover a large part of the field of electric machines and drives. Various types of electric machines, including three-phase and single-phase induction machines or doubly fed machines, are addressed. Most of the chapters focus on modern control methods of induction-machine drives, such as vector and direct torque control. Among others, the book addresses sensorless control techniques, modulation strategies, parameter identification, artificial intelligence, operation under harsh or failure conditions, and modelling of electric or magnetic quantities in electric machines. Several chapters give an insight into the problem of minimizing losses in electric machines and increasing the overall energy efficiency of electric drives.

How to reference

In order to correctly reference this scholarly work, feel free to copy and paste the following:

Omar Hegazy, Amr Amin, and Joeri Van Mierlo (2011). Swarm Intelligence Based Controller for Electric Machines and Hybrid Electric Vehicles Applications, *Electric Machines and Drives*, Dr. Miroslav Chomat (Ed.), ISBN: 978-953-307-548-8, InTech, Available from: <http://www.intechopen.com/books/electric-machines-and-drives/swarm-intelligence-based-controller-for-electric-machines-and-hybrid-electric-vehicles-applications>

INTECH
open science | open minds

InTech Europe

University Campus STeP Ri
Slavka Krautzeka 83/A
51000 Rijeka, Croatia
Phone: +385 (51) 770 447
Fax: +385 (51) 686 166
www.intechopen.com

InTech China

Unit 405, Office Block, Hotel Equatorial Shanghai
No.65, Yan An Road (West), Shanghai, 200040, China
中国上海市延安西路65号上海国际贵都大饭店办公楼405单元
Phone: +86-21-62489820
Fax: +86-21-62489821

© 2011 The Author(s). Licensee IntechOpen. This chapter is distributed under the terms of the [Creative Commons Attribution-NonCommercial-ShareAlike-3.0 License](#), which permits use, distribution and reproduction for non-commercial purposes, provided the original is properly cited and derivative works building on this content are distributed under the same license.

IntechOpen

IntechOpen